REPORT ON THE MINERAL EXPLORATION IN THE RAKAH AREA, SULTANATE OF OMAN

FINAL REPORT

VOLUME I (EXPLORATION RESULTS)

FEBRUARY 1990

JAPAN INTERNATIONAL COOPERATIONAL AGENCY
METAL MINING AGENCY OF JAPAN

REPORT ON THE MINERAL EXPLORATION IN THE RAKAH AREA, SULTANATE OF OMAN FINAL REPORT VOLUME I (EXPLORATION RESULTS) FEBRUARY 1990 JICA MMAJ

REPORT
ON
THE MINERAL EXPLORATION
IN
THE RAKAH AREA,
SULTANATE OF OMAN

FINAL REPORT

VOLUME Ⅱ
(EXPLORATION RESULTS)

FEBRUARY 1990

JAPAN INTERNATIONAL COOPERATIONAL AGENCY
METAL MINING AGENCY OF JAPAN

PREFACE

In response to the Government of the Sultanate of Oman, the Japanese Government decided to conduct a Preliminary Feasibility Study for Mine Development Project in Rakah Area and entrusted the survey to Japan International Cooperation Agency (JICA) and Metal Mining Agency of Japan (MMAJ).

The JICA and MMAJ sent to the Sultanate of Oman a survey team for two field seasons from 1988 to 1989, headed by Mr. Takehiko Nagamatsu. The team exchanged views with the officials concerned of the Govenment of the Sultanate of Oman and conducted a field survey in the Rakah area. After the field survey, further studies were made and present reports have been prepared.

The reports consist of three volumes. The summary of the work, exploration results and the preliminary feasbility study for mine development are given in Volume I, II and III respectively.

We hope that this report will serve for the development of the project and contribute to the promotion of friendly relations between our two countries.

We wish to express our deep appreciation to the officials concerned of the Government of the Sultanate of Oman for their close cooperation extended to the team.

February, 1990

Kensuke Yanagiya
President
Japan International Cooperation Agency

Gen-ichi Fukuhara
President
Metal Mining Agency of Japan

VOLUME II

CONTENTS

Chapter 1 Area A (Hayl as Safil deposit)

1-1 General

In order to clarify the potential and nature of the mineralized zones, geologic, geophysical (CP method) and drilling surveys were carried out in the period of two years in this project.

The work methods and amounts completed in this project in Area A are given below.

Geologic survey: 3 km^2, 1:2,000 in scale
Geophysical survey: Charged potential (CP) method, 611 stations
Drilling: 12 holes, 1,740.80 m in total

These survey results clarified the geology and geologic structure of Area A, and also the Hayl as Safil deposit was clearly delineated.

1-2 Geologic survey

1-2-1 Geology

(1) General geology

The Oman Mountains, forming a part of the Alps-Himalaya orogenic belt, consist of autochtonous and allochthonous units. The autochtonous units form the Arabian Platform and are the Pre-cambrian to Mesozoic formations. The allochthonous units, overthrusted onto the autochtonous units, consist of Hawasina Nappes and overlying Samail Nappe. The Hawasina Nappes are made up of Hawasina Sediments and the Samail Nappe is divided into Samail Ophiolite and Supra-ophiolite Sediments.

The Rakah area including Area A and B is situated at southwestern flank of the central part of the Oman Mountains. Geology of the area consists of the Samail Ophiolite including Tectonites, Cumulate Sequence, High-level Gabbro, Sheeted-dyke Complex and Samail Volcanic Rocks in ascending order, and the Supra-ophiolite Sediments (Fig. 1-1). Tectonostratigrapohic section is shown in Fig. 1-2.

Area A is situated in the west part of the Rakah area. Geology in the area consists of the Samail Ophiolite and Supra-ophiolite Sediments. Outcrops of these rocks are limited and scattered because of widespread thick terrace deposits. The geologic maps for Area A are given in Fig. 1-3 and Plate II-1-1, and the cross sections are given in Plate II-1-2.

Tectonically, the area is marked by two thrust faults trending an E-W direction. These thrust faults are found in the eastern part of the area. The area is also characterized by imbrication

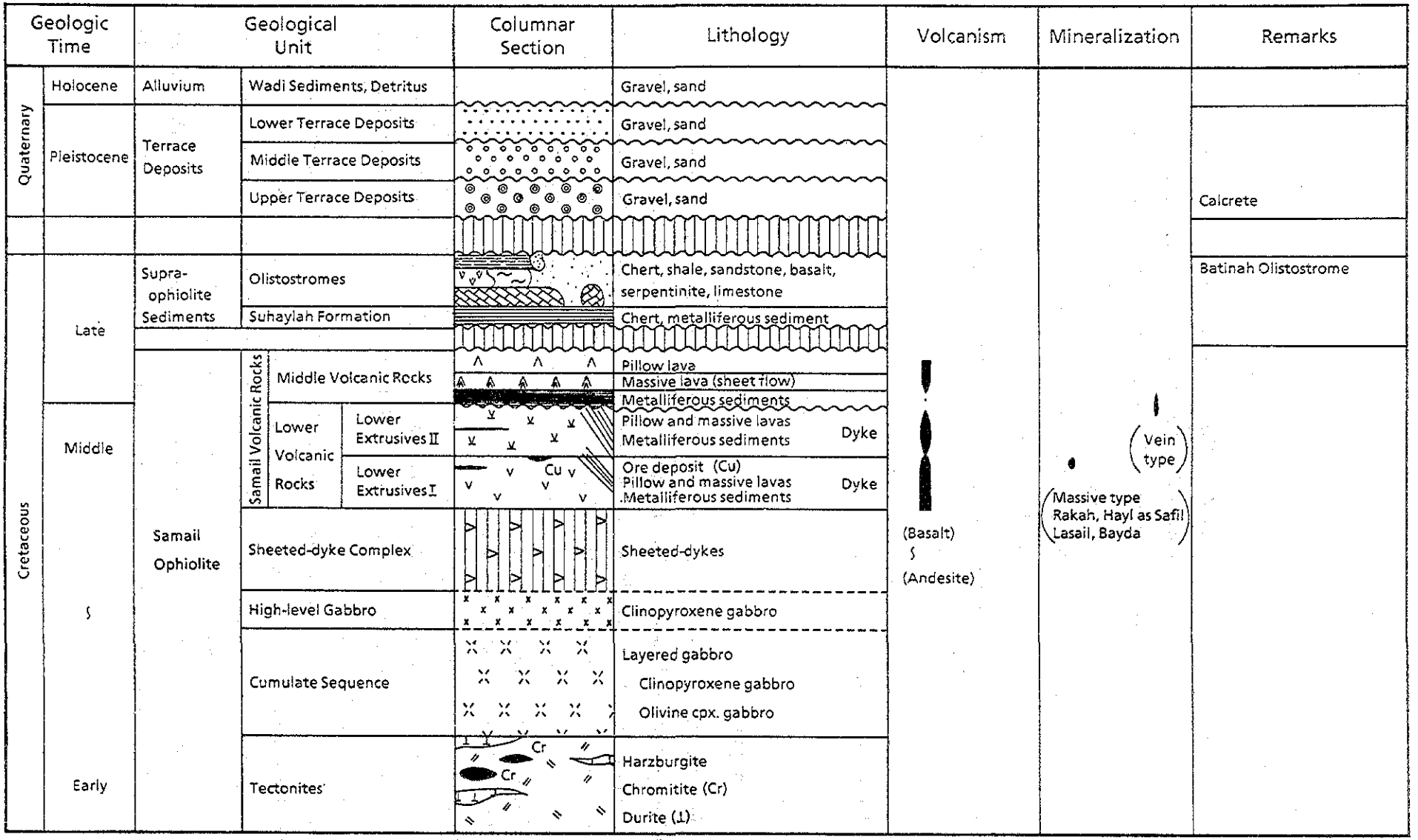

Fig. 1-1 Stratigraphic columnar section of the Rakah area

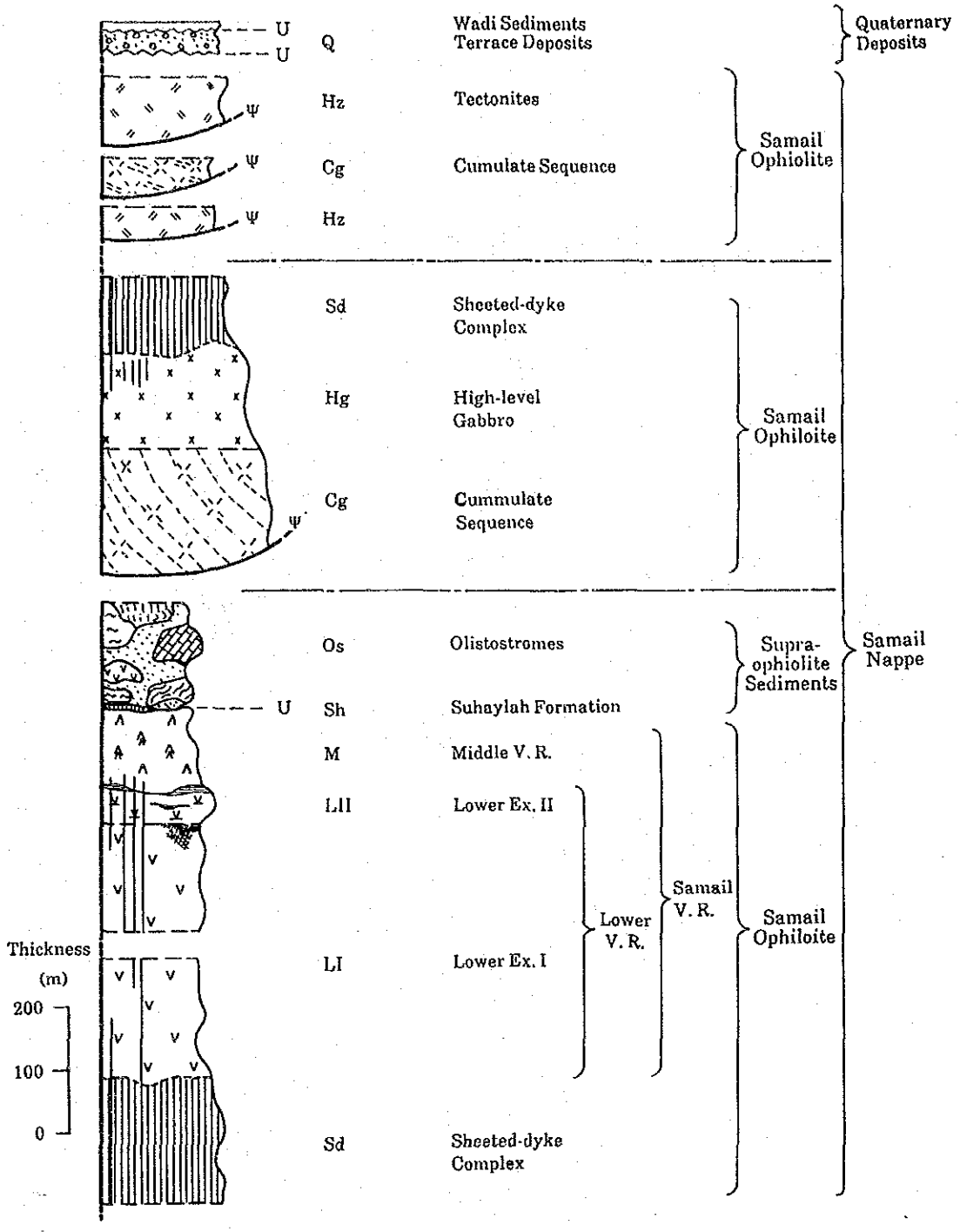

Ψ	:	Thrust fault	Q	:	Quaternary	Sd	: Sheeted-dyke Complex
U	:	Unconformity	Os	:	Olistostromes	Hg	: High-level Gabbro
V.R.	:	Volcanic rocks	Sh	:	Suhaylah Formation	Cg	: Cumulate Sequence
Ex.	:	Extrusives	M	:	Middle Volcanic Rocks	Hz	: Harzburgite
			LII	:	Lower Extrusives II		
			LI	:	Lower Extrusives I		

Fig. 1-2 Tectonostratigraphic section of the Rakah area

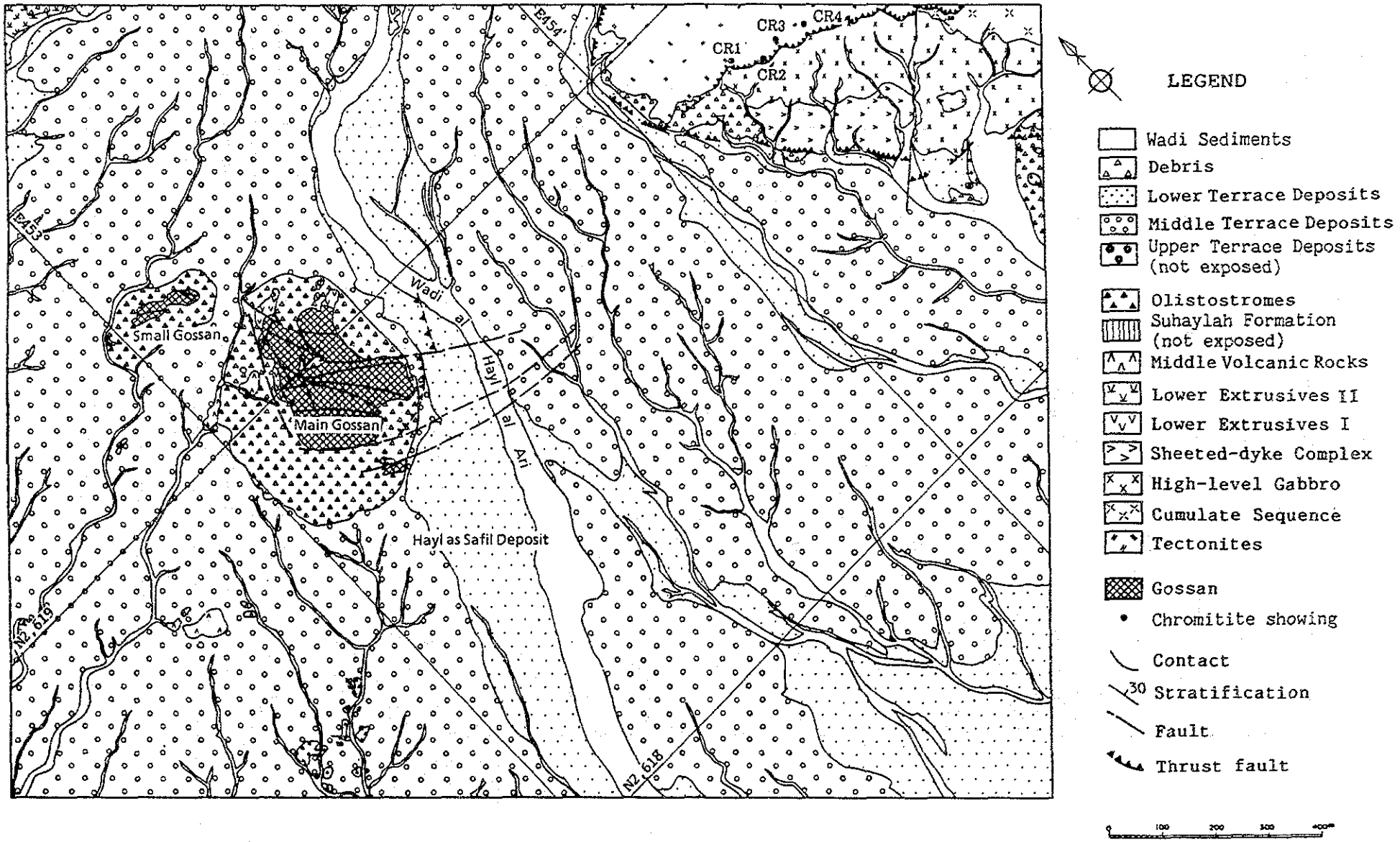

Fig. 1-3 Geologic map of Area A

structure and stratigraphically lower units of ophiolite can be observed at the upper part. Two fault systems of NW-SE and NE-SW are found in the area (Fig. 1-4).

(2) Stratigraphy

Results of microscopic observation are shown in Table 1-1 and Appendix 1.

(i) Samail Ophiolite

The Samail Ophiolite in the area consists of Tectonites, Cumulate Sequence, High-level Gabbro, Sheeted-dyke Complex and Samail Volcanic Rocks in ascending order.

(a) Tectonites

The Tectonites form a mountainous zone in the northeastern corner of the area with an E-W direction. The rocks consist of harzburgite with subordinate dunite, gabbro, chromitite and orthopyroxenite dyke. The Tectonites show a WNW-ESE direction as a whole, but internal structures are generally invisible. The rocks have more than 80 m thick in the area. The relationship between the Tectonites and Cumulate Sequence is fault contact.

Harzburgite (Hz)

Harzburgite is dark brown to dark green and is composed of olivine and bastitized orthopyroxene. A banded structure is observed in places in the lower part of the Tectonites. The rock is marked by strong serpentinization. Foliation is generally invisible, but is weak. Foliation striking NNW-SSE and dipping 60° to the east, is measured in the west part of the Tectonites. Numerous magnesite veins, ranging in thickness from 1 cm to 10 cm and in strike length from 1 m to 5 m, are found in the Tectonites. These veins strike N 60° ~ 80° W and dip steeply to the east.

The lowest part of the Tectonites is sheared along a thrust fault with width of several meters. (Fig. 1-5).

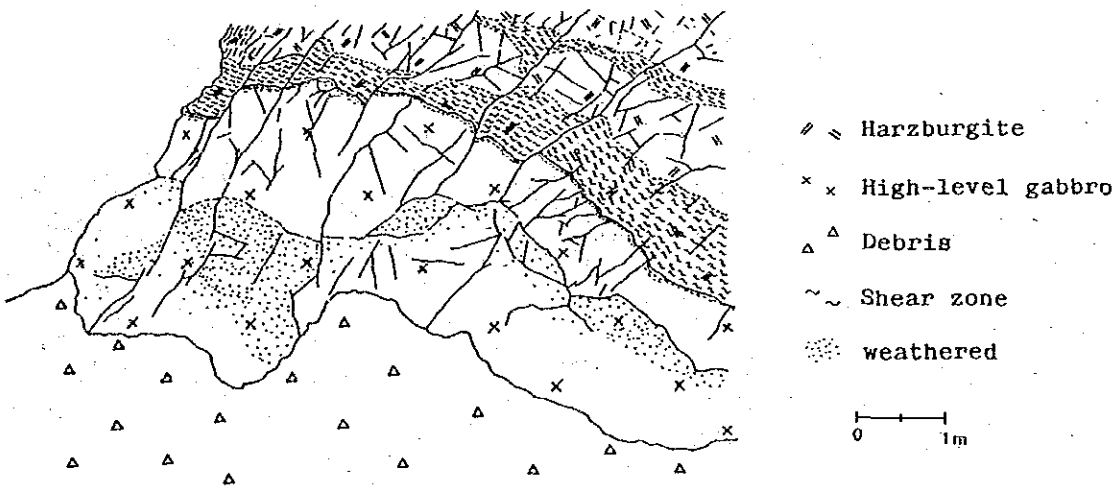

Fig. 1-5 Sketch of thrust fault between Tectonites and High-level Gabbro

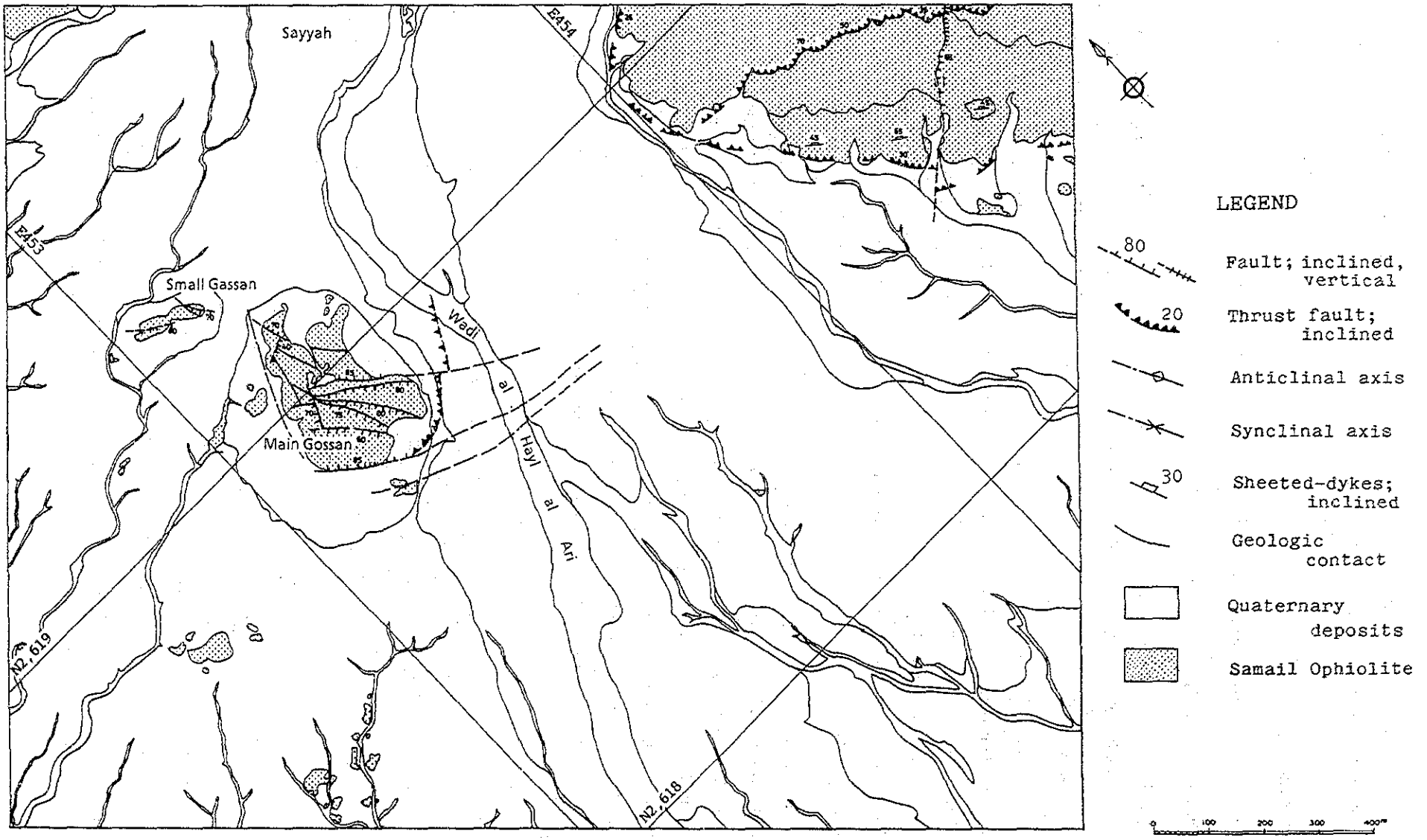

Fig. 1-4 Structural map of Area A

Table 1-1 Observation results of thin sections

Ser. No.	Sample No.	Coodinates N (km)	Coodinates E (km)	Geol. Unit	Rock Name	Texture	Phenocrysts Qz	Ne	Ap	P	Kp	Pl	Bi	Ho	Au	Hy	Ol	Cr	Op	Groundmass Qz	Pl	Bi	Ho	Hy	Au	Ol	Mt	Op	Gl	Secoundary Minerals Qz	Ab	Sr	Cc	Cl	Ep	Ho	Zo	Sh	Pr	Tr	Sm	Se	Lm	Hm	Op	Remarks
1	M003	2,618.723	453.108	Me	basalt	intergranular						○			○						◎			•	●			●						◎	○	○					○					●	Ti-augite
2	M005	2,619.150	452.857	Me	dolerite	ophitic						◎			○				●		○				○			●						◎	○	○			•			○					
3	M011	2,618.724	454.245	Hg	hb-cpx gabbro	porphyritic			•			◎		○	○				●		○									○		○		○	○	○		●		●				•		
4	M012	2,618.638	454.222	Sd	dolerite	–						○																					●	○	◎			•							●	altered
5	M015	2,619.830	453.344	LII	andesite	glomeroporphyritic						○			●				●		○								○						○	◎						○			•		devitrification
6	M016	2,617.975	457.542	Sd	andesite	intergranular						◎									○				●			●						○	○	○			●								altered
7	M017	2,618.985	457.200	Cg	cpx gabbro	ortho-cumulate			•			◎			○				●												○	●	●		○											poikilitic
8	M018	2,618.950	457.236	L'	andesite	–																								◎			◎	◎			●					•		●	altered
9	M020	2,618.365	457.172	LII	basalt	hyalopilitic									○				●										○	○			○	○			●			○						devitrification
10	M022	2,618.938	458.642	Me	andesite	ophitic						◎			○													●		○		○	○	◎	○					○					●	
11	M023	2,618.440	458.925	Me	basalt	intergranular						○			○						○					●		●					●	◎	○	○			●							
12	M024	2,618.314	458.596	LI	basalt	intersertal						○									◎				○			●	○			●	○	○	○			●								argillization
13	M031	2,618.269	457.534	L'	dolerite	subophitic						○			○						○				○			●				◎	○	○	●			●							
14	M032	2,617.977	457.502	LI	andesite	intersertal						●							●											○			●	◎	○			●			○				
15	M034	2,619.127	453.198	LI	andesite	–						●																		◎				○				●			○			●	altered
16	MJO-A4 44.20	2,618.676	453.458	LII	andesite	intersertal						●			●						◎				○			●	●			●	◎				•				•				brecciated
17	MJO-A4 143.70	2,618.676	453.458	LI	basalt	intersertal, vesicular									●						○				◎			●	○			●	◎	○		○	•							○	
18	MJO-A1 63.70	2,618.742	453.434	LII	basalt	intersertal									○						◎				○			●	○	○				◎	●										
19	MJO-A1 172.00	2,618.742	453.434	LI	basalt	variolitic, vesicular									●						●				○			•		○				◎				•	●		○					chloritization
20	MJO-B5 23.50	2,618.700	457.404	LII	basalt	hyalopilitic									●						●				○				●	○			○	○										○	
21	MJO-B5 79.20	3,618.700	457.404	LI	basalt	hyalopilitic									●						●					●			○	◎			○	○				•							○	
22	MJO-B5 136.10	2,618.700	457.404	LI	basalt	intersertal						●			●						◎				○			●		○				◎	○			●								
23	MJO-B3 55.20	2,618.784	457.526	LII	basalt	intersertal, vesicular									○						◎				○			●		○				○	○			•	○							
24	MJO-B3 147.70	2,618.784	457.526	LI	basalt	intrsertal						●			●						○				○			●						○	◎	○			●				●	●		chloritization
25	MJO-B4 101.20	2,618.723	457.358	LI	basalt	hyalopilitic									○						●				○					○				○	◎	●										chloritization
26	MJO-B6 85.90	2,618.631	457.405	LI	basalt	intersertal						○			●						◎				○				•	○				○	◎	●			●							●	chloritization
27	N011	2,618.782	453.194	LII	andesite	variolitic									○						●				○				●	◎				○									●		○	*silicification*
28	MJO-B2 52.20	2,618.772	457.385	LII	andesite	hyalopilitic									●						●				○				○	◎				●	◎	●										●	
29	MJO-E3 125.90	2,618.770	457.526	LI	basalt	–																								◎				○	◎			●						●	○	altered
30	MJO-A5 17.50	2,618.796	453.299	LII	basalt	intergranular						◎			○						◎				○				●	●				◎	●			•			○					
31	MJO-A12 81.00	2,618.680	453.637	LII	basalt	intersertal									○						◎				○			•	●	•				◎			•		•							
32	MJO-A12 99.80	2,618.690	453.637	LI	basalt	intersertal															◎				○			•	•	•			○	◎			●			○					•	
33	MJO-A10 58.90	2,618.795	453.200	LI	basalt	glassy									○		○							○	◎	?		•	◎					○						○						
34	MJO-B9 14.30	2,618.765	457.334	LII	basalt	glassy									◎										•			•	◎										◎							
35	MJO-B9 50.00	2,618.765	457.335	LII	basalt	glassy									◎										○			•	◎	•				○					○							
36	MJO-B9 120.00	2,618.765	457.335	LI	basalt	glassy									◎										○			•	◎	•				○			•		•	○						

◎ abundant ○ common ● rare • very rare

Me : Middle Volcanic Rocks
LII : Lower Extrusives II
LI : Lower Extrusives I
Sd : Sheeted-dyke Complex
Hg : High-level Gabbro
Cg : Cumulate Gabbro
L' : Late dykes

Ab : *albite*
Ap : apatite
Au : augite
Bi : biotite
Cc : calcite
Se : *sericite*
Cl : chlorite
Cr : chromite
Ep : epidote
(Gl) : (glass)
Mt : *magnetite*
Ne : nepheline
Ol : olivine
Op : opaque minerals
Pl : plagioclase
Pr : prehnite
Qz : quartz
Sh : sphene
Sm : smectite
Sr : sericite
Tr : tremolite
Zo : zeolite

Dunite (Du)

Dunite is found as small lenticular bodies in harzburgite. The bodies range in thickness from 1 m to 10 m and in length from several to a hundred meters. They strike N 10° ~ 40° W and dip 30° to the east. The boundary between dunite and harzburgite is not clear and gradational change is observed in some places. Four chromitite showings were found within the dunite.

Chromitite (Cr)

Four chromitite (Cr) showings were discovered in Area A. These showings were found in the lower part of Tectonites. Chromitite shows gradational change to dunite and has fault contact with harzburgite. Gabbro is locally accompanied with chromitite. Chromitite bodies show lenticular shape and 3 m in width and several meters to 20 m in length. Chromite ore is compact and massive to disseminated ores. Fig. 1-6 shows the occurrence of chlomitite.

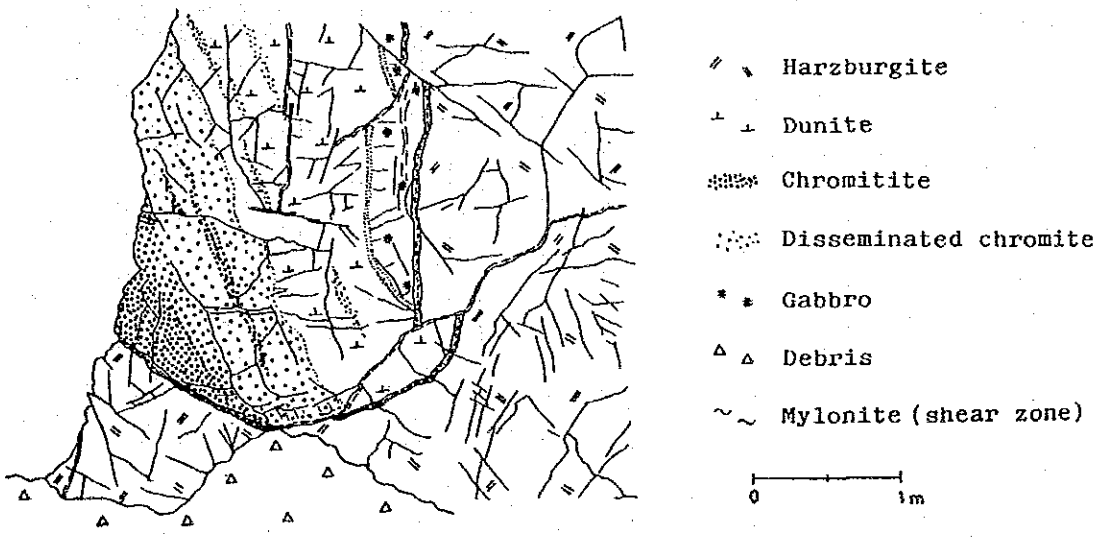

Fig. 1-6 Sketch of chromitite showing

Four samples were collected from the chlomitite outcrops and assayed in the laboratory of MPM. The results are as follows:

Sample number	Cr_2O_3 (%)	SiO_2 (%)	FeO_3 (%)	CaO (%)	Al_2O_3 (%)	MgO (%)
CR 1	30.5	14.9	13.8	3.36	16.1	21.18
CR 2	28.3	22.1	13.8	4.18	12.4	21.15
CR 3	33.6	11.6	15.3	2.31	17.0	20.15
CR 4	34.2	9.8	15.0	1.43	17.7	20.83

The sampling sites are shown in Fig. 1-3.

Orthopyroxene Gabbro (Ga)

The rocks are found locally in harzburgite. The bodies show small lenticular or oval shape ranging in width from several tens centimeters to one meter. They trend NW-SE in general and dip 40° to 60° NE. Harzburgite surrounding the clinopyroxene gabbro is marked by serpentinization and the boundary between these two rocks are not clear.

Orthopyroxenite (D')

The rock is obseved as dykes in harzburgite. The dykes show irregular and undurate shape, and have width ranging from several centimeters to several tens centimeters. The dykes strike NW-SE to NNW-SSE and consist of greenish gray and coarse-grained orthopyroxene.

(b) Cumulate Sequence (Cg)

The rocks are found locally in the eastern edge of the area, and have a thrust fault contact with Tectonites. The rocks are more than 150 m thick and show gradational change to upper unit of the High-level Gabbro.

The rocks consist of clinopyroxene gabbro with subordinate olivine gabbro. Because of different contents of maffic minerals, the gabbro present distinct layered structure ranging in width from several milimeters to several tens centimeters. The layering strikes N-S to NNW-SSE and dips 30° to 50° eastward.

The clinopyroxene gabbro is light greenish gray to dark gray and shows medium- to coarse-grained texture. Clinopyroxene forms lamination in the rock. The olivine gabbro has a 20 cm to 30 cm in thickness and is dark brownish green. Olivine in the olivine gabbro altered to serpentine and limonite, and shows brownish gray in color. Pyroxene is also altered mostly to chlorite. Numerous veinlets of prehnite, carbonates and epidote etc. are found in this unit.

(c) High-level Gabbro (Hg)

High-level Gabbro (Hg) occurs in the eastern part of the area and the thickness is 100 m to 150 m. This unit is overlain the Cumulate Sequence with gradational contact and is underlain the Sheeted-dyke Complex with transition zone of about several tens meters. Numerous dykes of dolerite and basalt ranging in width from 30 cm to 1 m intrude in the upper part of the unit. Dolerite stocks of 5 m to 10 m wide are also found locally in the unit.

The unit consists of light greenish gray to greenish gray clinopyroxene gabbro with subordinate hornblende-bearing gabbro. It shows fine-grained texture in the upper part and medium to coarse-grained texture in the lower part. Gabbroic pegmatite with several meters wide are found in places in the lower part. Chloritization and epidotization are observed in the unit, especially along dykes. Weak mineralized zones with hematite, limonite and green copper minerals and argillized zones are also locally observed.

(d) Sheeted-dyke Complex

The Sheeted-dyke Complex is found locally in the eastern part of the area. The relation with the underlying High-level Gabbro is gradational and the upper part is cut by faults. This unit is estimated at least more than 100 m thick.

More than 70% of the unit is composed of dark gray and greenish gray dolerite to basalt and basaltic andesite. The dykes generally strike N 40°~70° W and dip 35° ~ 75° to the north. The dykes have chilled margin of serveral centimeters wide. Width of each dyke ranges from 30 cm to 1 m. Fine-grained clinopyroxene gabbro occurs in the matrix of the lower part. Strong epidotization is recognized in the unit.

A shear zone with several meters wide is found in the southwestern edge of the exposure. The shear zone trends a NW-SE direction and dips 30° NE which is a possibly thrust fault. Pillow lavas and dykes are observed beneath the shear zone and the rocks may correspond to the lower part of the below-mentioned Samail Volcanic Rocks.

(e) Samail Volcanic Rocks

The Samail Volcanic Rocks can be divided into Lower Volcanic Rock, Middle Volcanic Rocks and Upper Volcanic Rocks (Bishimetal, 1987) in ascending order. The Lower and Middle Volcanic rocks are found in the survey area. The Lower Volcanic Rocks can be subdivided into Lower Extrusives I and Lower Extrusives II based on the different nature of pillow lavas. Stratigraphic correlation of Samail Volcanic Rocks between the northern part of the Oman Mountains and the Rakah area including Area A and B is shown in Fig. 1-7. Columnar sections along survey route in Area A are shown in Fig. 1-8.

Lower Extrusives I (LI)

The rocks are found in the northwestern corner and northern immediate flank of Main Gossan. The weakly altered Lower Extrusives I shows dark greenish gray to light brownish green in color, but the strongly altered zone shows dark green to light brown and no volcanic texture can be observed. The rocks consist of pillow lavas with subordinate massive lavas. Pillow shows oval shape with diameter ranging from 60 cm to 100 cm. Some vesicles are observed and are filled with calcite and quartz. Hyaloclastite which forms matrix of pillow is 2 cm to 3 cm in thickness and is accompanied with subordinate pillow breccia.

Lower Extrusives II (LII)

The rocks are found locally in the north corner of the area and south of Main Gossan. The thickness of this unit is more than 20 m. The rocks are purplish gray to light greenish gray and consist of pillow lavas and subordinate massive lavas. Diameter of pillow ranges from 30 cm to 60 cm and has an amygdaloidal texture filled with zeolites, calcite, epidote and chlorite. Hyaloclastite around the pillow is relatively thin and ranges in thickness from 1 cm to 3 cm.

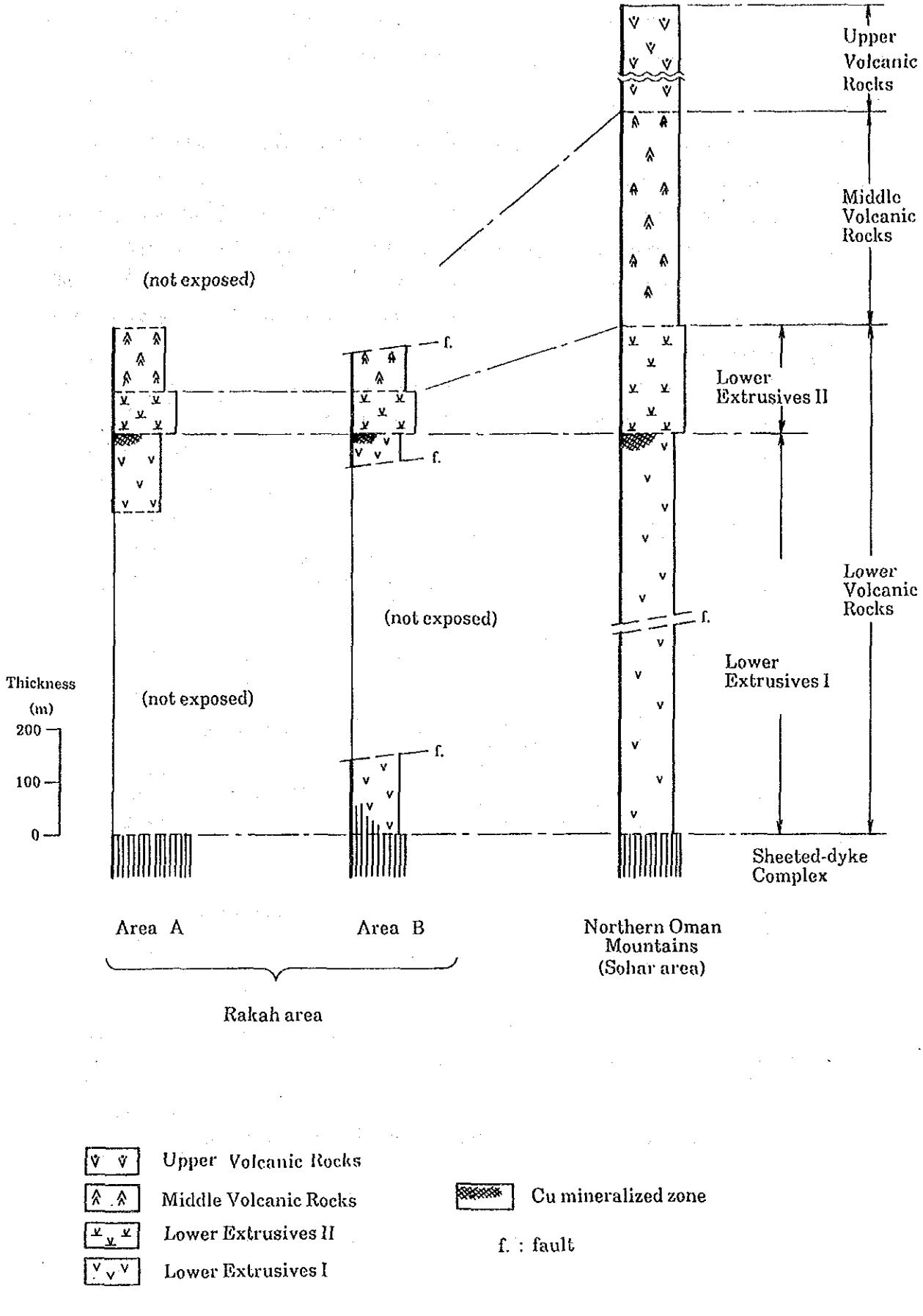

Fig. 1-7 Correlation of Samail Volcanic Rocks in the Oman Mountains area

Three metalliferous sedimentary layers are found in this unit. These are reddish brown in color and up to 3 cm in thickness. The layers strike N 20° ~ 40° E and dip 30° to 40° toward east.

Middle Volcanic Rocks

The Middle Volcanic Rocks are found in the west of the Main Gossan and consist of extrusive rocks and metalliferous sedimentary layers. The extrusives are composed of dark greenish gray to greenish gray pillow lavas (Me) and massive lavas (Mms). Small but typical outcrop of the pillow lavas is found in the southeastern part of the area. The pillows are relatively large ranging the diameter from 0.6 m to 1.2 m and show irregular oval shape. The massive lavas occur at the west to southwest of Main Gossan and consist of fine to medium-grained dolerite containing chloritized pyroxene as the phenocryst.

The metalliferous sedimentary layers are interbedded in the massive lavas. The layers are dark reddish brown and have thickness ranging from 5 cm to 12 cm.

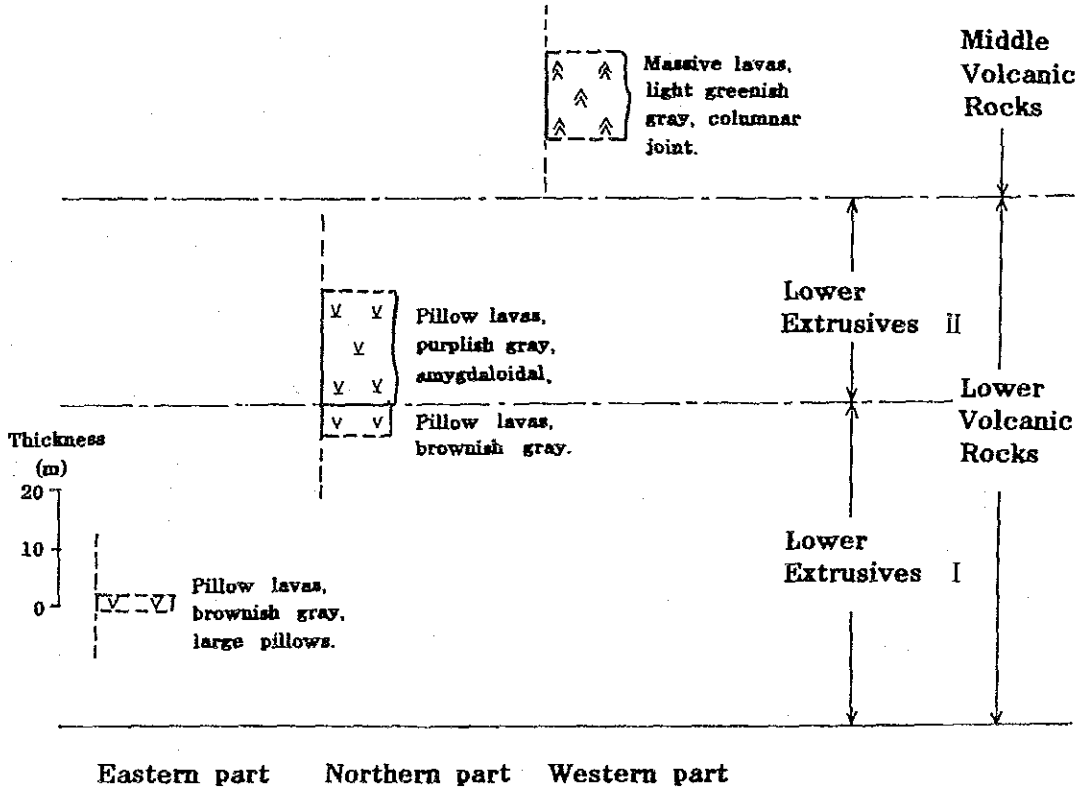

Fig. 1-8 Columnar sections of volcanic rocks in Area A

(ii) Supra-ophiolite Sediments

This unit is found locally in the eastern and southwestern parts of the area and consists of Olistostrome (Os). The Olistostrome presents chaotic structure and contains various kind of olistoliths including red chert, reddish brown siliceous shale, dirty limestone, basalt and bedded limestone etc.

Individual olistoliths show the size ranging from several tens meters to several hundreds meters. The relationship between the Olistostrome and Samail Ophiolite is unknown because of no outcrops of the contact in the area.

(iii) Quaternary

Quaternary superficial deposits are divided into terrace deposits, debris and wadi sediments.

(a) Terrace Deposits (Qt.)

Terrace is widespread in the area and is divided into middle and lower terraces. Upper terrace found in Area B is not observed in this area.

The middle terrace is between 680 m and 720 m above sea level and is distributed widely in the area. Middle Terrace Deposits (Qtm) forming the middle terrace consist of sand and gravel, and reach the thickness up to 40 m. The gravels are mostly rounded to subrounded gabbro and harzburgite ranging the diameter from 1 cm to 60 cm. The deposits are ill sorted and occasionally intercalate thin fine to coarse-grained sand beds. The bottom of the deposits consist of granule to coarse sand and area mostly cemental with carbonate.

The lower terrace is situated between 675 m and 710 m above sea level and occurs along the main wadis and the surroundings. The level of middle terrace is higher from 3 m to 8 m than that of lower terrace. Lower Terrace Deposits (Qtl) are similar to those of the Middle Terrace Deposits (Qtm).

(b) Debris (Qd)

Debris occurs at the northeastern part of the area and the surroundings of Main Gossan and Small Gossan. The Debris (Qd) in the gossan zones has several meters thick and consists of angular gravel of siliceous gossan ranging in diameter from 1 cm to 50 cm..

(c) Wadi Sediments (Qw)

The Wadi Sediments (Qw) are found along wadis and consist of rounded to subrounded gravels with diameter from 1 cm to 30 cm. The gravels are mostly gabbro and harzburgite.

(iv) Intrusive Rocks

Basaltic to andesitic dykes are found in the eastern end of the area. The dykes are dark green to greenish gray and have chilled margin with width of 2 to 3 cm. The rocks are altered and

contain epidote and carbonate veinlets. The dykes have width ranging from 30 cm to 2 m and have a direction of NW-SE dipping 30° to 50° toward northeast. The direction and dip of the dykes are similar to those in the Sheeted-dyke Complex. The dykes are possibly feeder dykes of the Lowe Volcanic Rocks.

1-2-2 Geologic structure

Tectonic history in the Rakah area can be divided into three stages. These are formation of Samail Ophiolite (first stage), obduction of Samail Ophiolite (second stage) and tectonic movement of post-obduction (third stage).

In the first stage, the Samail Ophiolite was formed in the spreading ridge of the Palaeo-Tethys sea during the Early to Middle Cretaceous time (Lippard et al., 1986), and Hawasina Basin was situated between the spreading ridge and the Arabian Plate, and formed the Hawasina sediments in the basin as shown each situation in Fig. 1-9 (1). Original structures within ophiolite are preserved generally in Sheeted-dyke Complex, Cumulate Sequence and Tectonites. The Sheeted-dyke Complex in Aera A and B shows original structure, which has a direction of NW-SE. This direction corresponds with the general trend of the Samail Ophliolite, which is found broadly in the Oman Mountains.

The second stage is related to the obduction of the Samail Ophiloite, after the obduction of Hawasina Nappe, onto the Oman Platform, which is located in southwestern edge of the Arabian Plate, following detatchment from sea-floor and deposition of the Supra-ophiolite Sediments. The obduction of Samail Ophiolite is considered to be of the Late Cretaceous age (Coleman, 1981 and Lippard et al., 1986) (Fig. 1-9 (2)). Thrust faults and folds trending NNW-SSE to NW-SE, which is related to the obduction, are found widely in the Oman Mountains. In the Rakah area, several thrust faults trending NW-SE to E-W are found. Although internal structures of the individual thrust sheets show normal stratigraphic sequence, upper part of the sequence is tectonically overlain by lower part of the sequence as just like reversed structure. This feature is thought to be imbricated structure resulted by the formation of several thrust faults (Fig. 1-9 (3), (4) and (5)).

The third stage is post-obduction and shows a variation in different localities. In Area A, two thrust faults trending NNW-SSE and dipping gently to the north, are found in the eastern part of the area. These thrust faults are situated between High-level Gabbro and Sheeted-dyke Complex in the upper part and between Sheeted-dyke Complex and Volcanic Rocks in the lower part. Faults consist of three directoions of faults, including N-S, NE-SW and NW-SE. Most of faults are high angle (70° ~ 90°), but low angle (40° ~ 50°) faults are inferred locally.

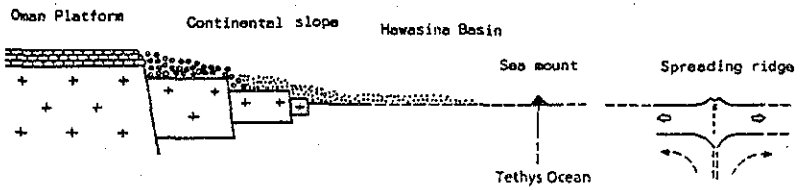

(1) Spreading ridge magmatism
(Formation of Samail Ophiolite)

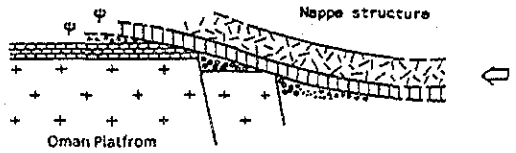

(2) Detachment and obduction of Samail Ophiolite

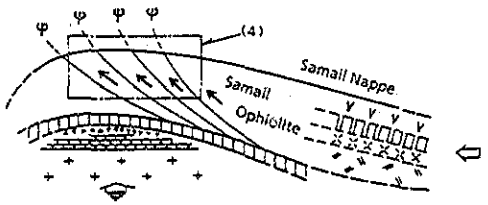

(3) Thrusting

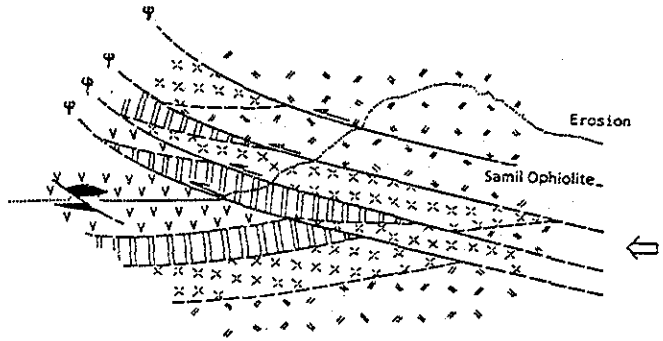

(4) Imbricated structure

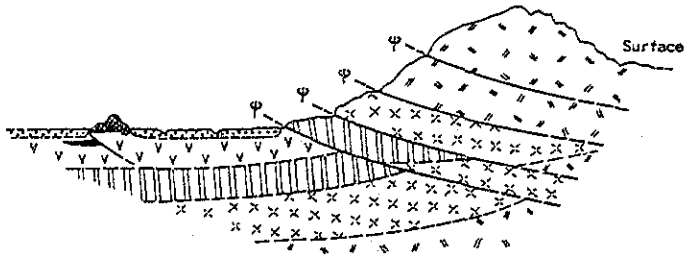

(5) Present profile

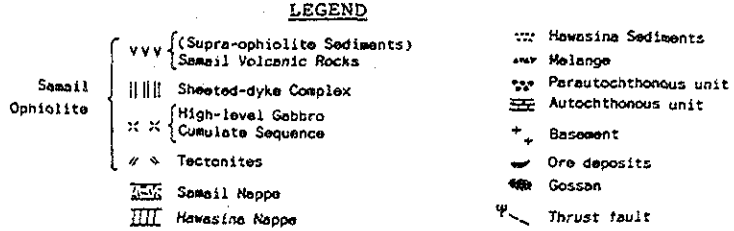

Fig. 1-9 Tectonic history of Samail Ophiolite in the Rakah area

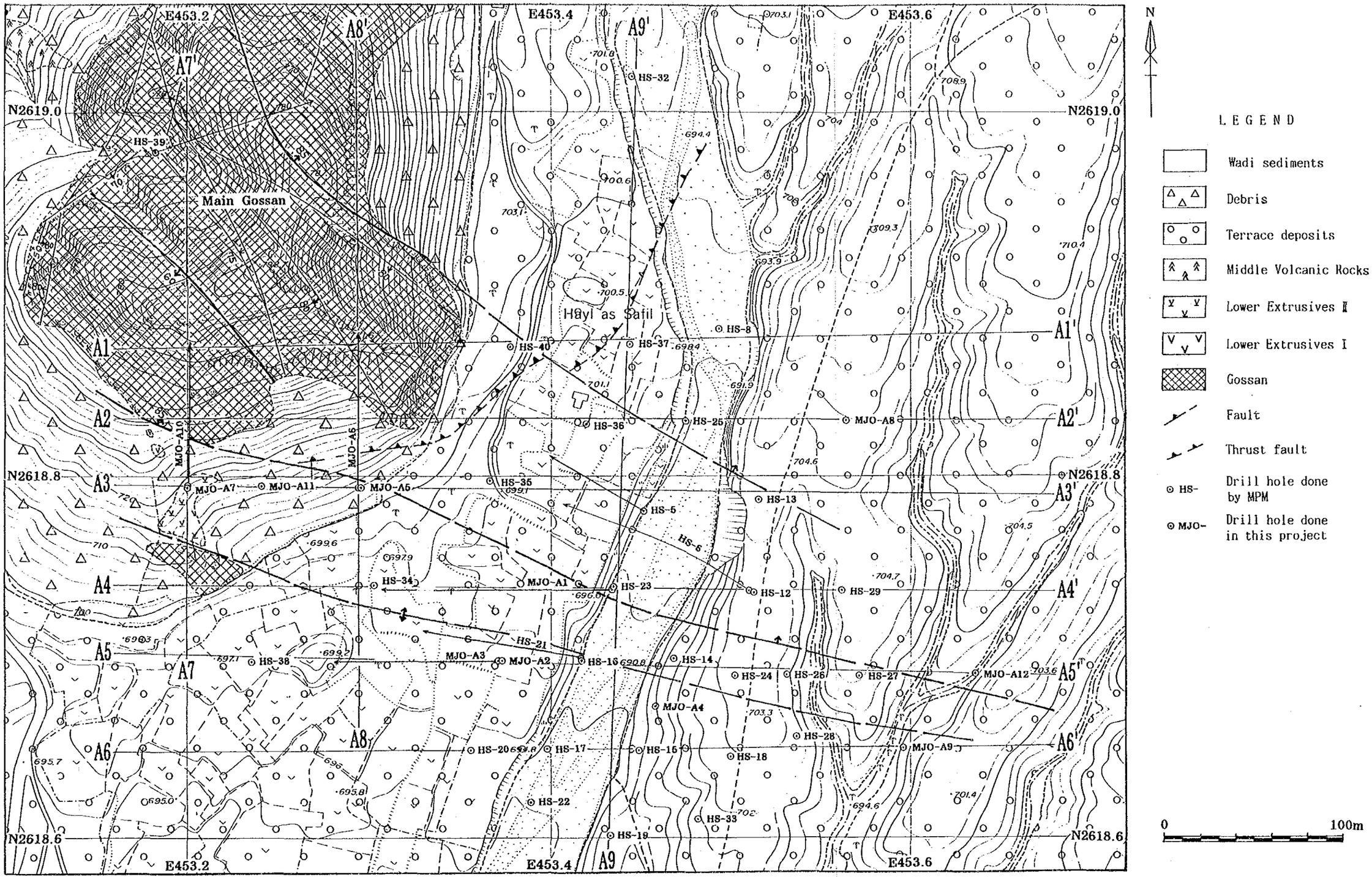

Fig. 1-10 Geologic map of the Hayl as Safil deposit area

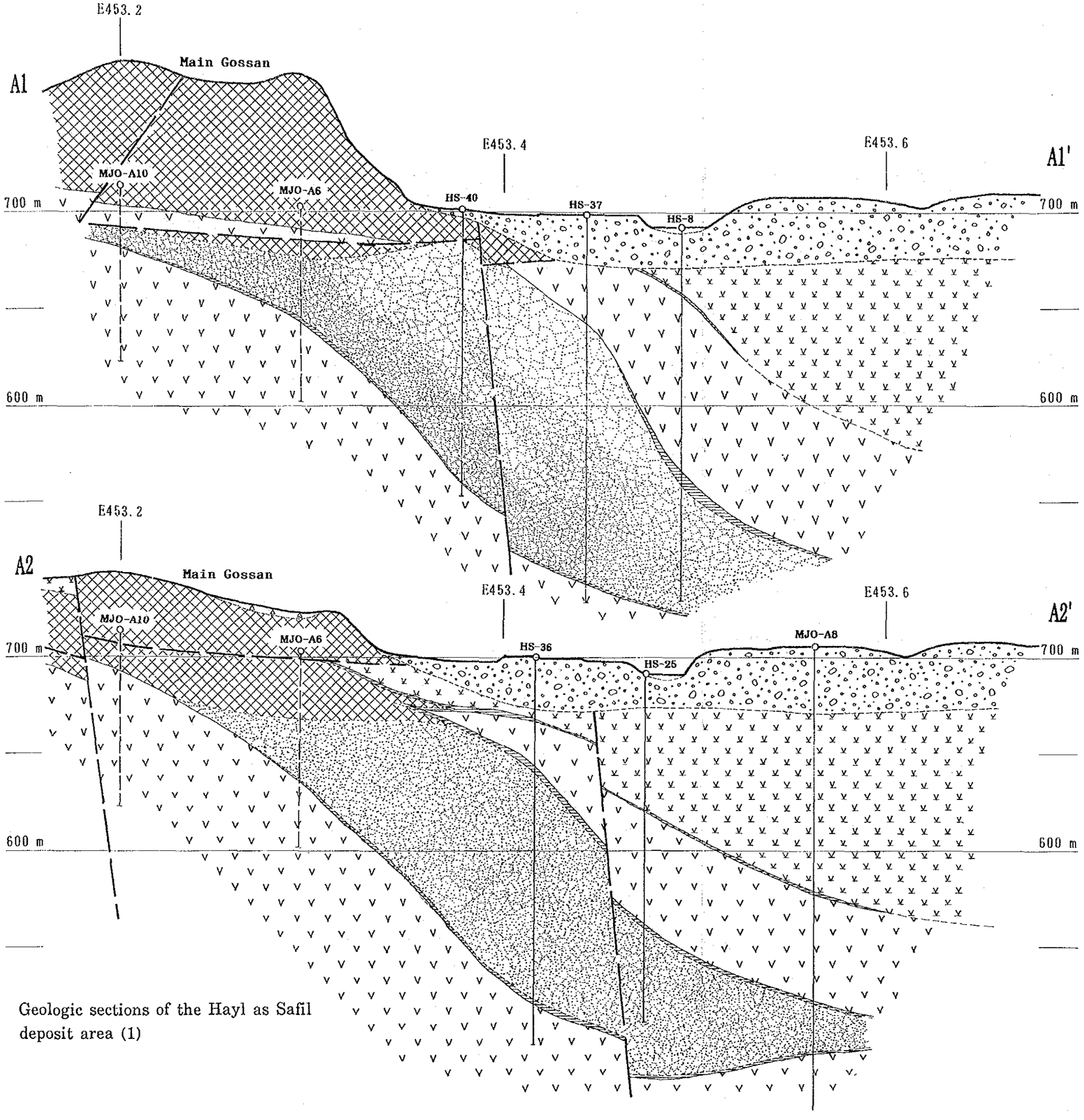

Fig. 1-11 Geologic sections of the Hayl as Safil deposit area (1)

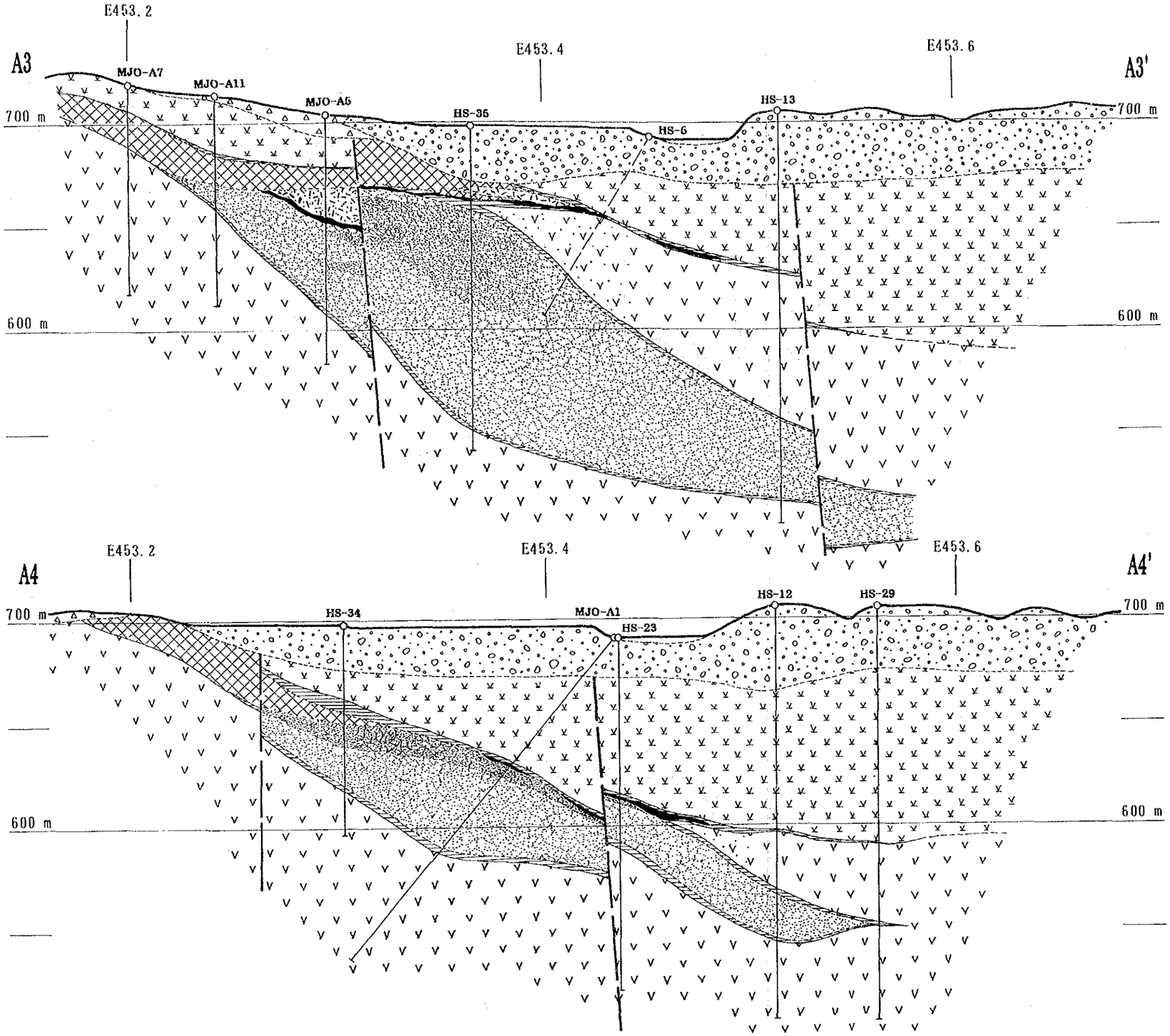

Fig. 1-11 Geologic sections of the Hayl as Safil deposit area (2)

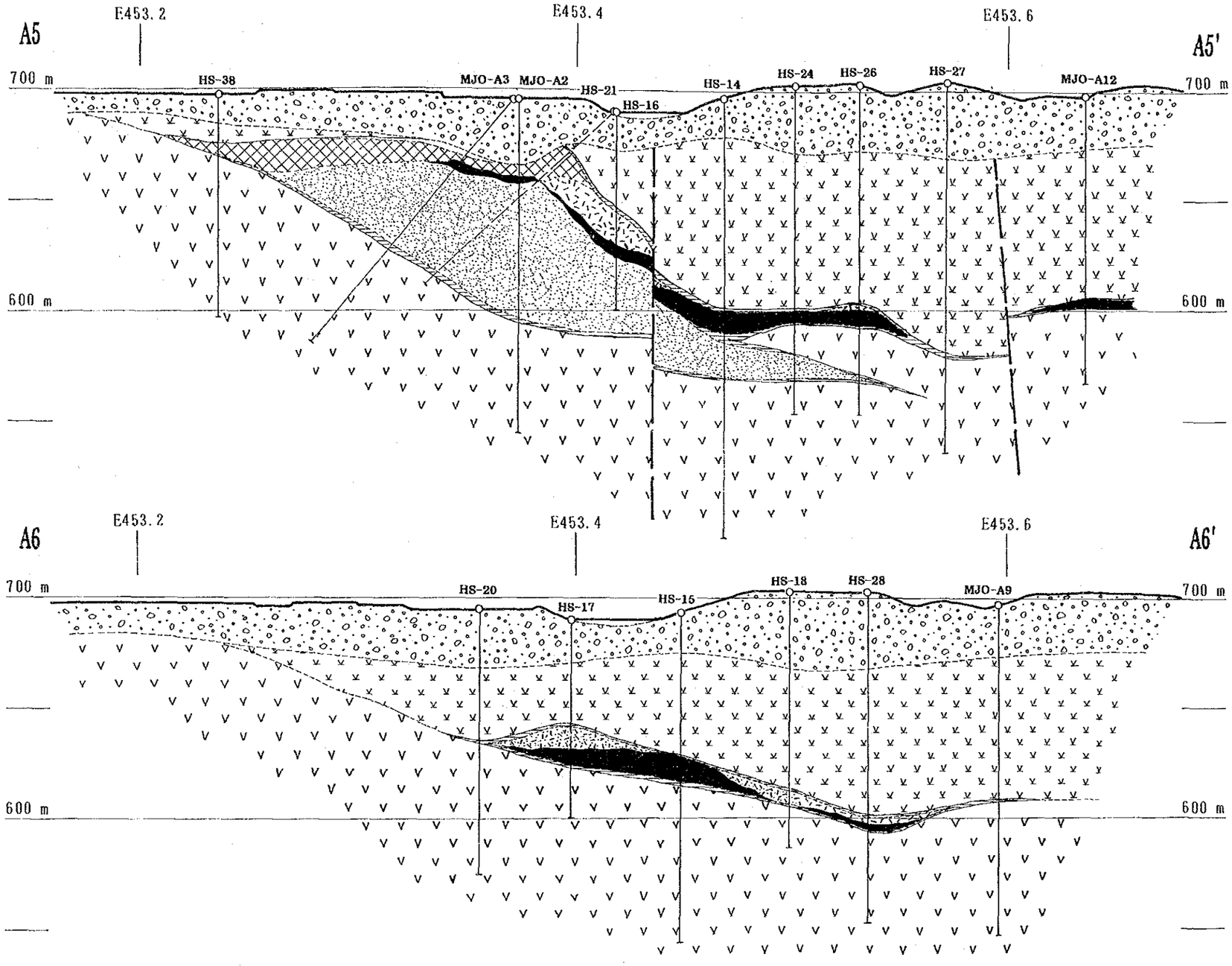

Fig. 1-11 Geologic sections of the Hayl as Safil deposit area (3)

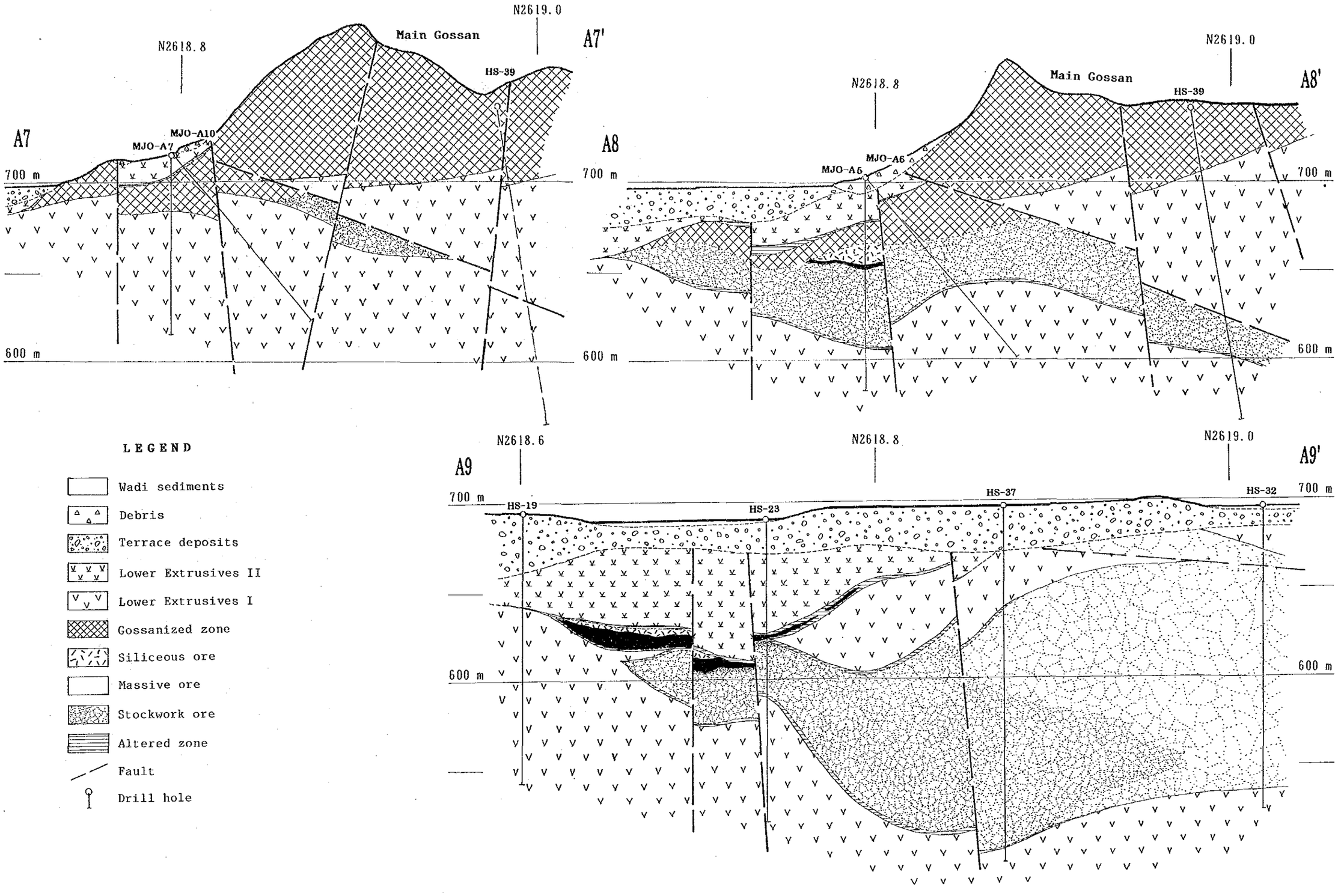

Fig. 1-11 Geologic sections of the Hayl as Safil deposit area (4)

1-2-3 Mineralization

(1) General of mineralization

Two intense gossanized zones outcrop in Area A. These are Main Gossan and Small Gossan. As the results of the previous drilling survey completed in Area A, two mineralized zones were discovered at southeast of Main Gossan and north of Small Gossan. Among these mineralized zones, the mineralized zone at the southeast of Main Gossan is the most significant one. Previous survey results were interpreted that Main Gossan and the mineralized zone at southeast were formed separately, and only this mineralized zone was called as the Hayl as Safil deposit.

The results obtained in this survey show that these mineralized zones including gossan zones were formed as one orebody and later fault movement and erosion separated them. Therefore, whole mineralized zones in Area A should be called as the Hayl as Safil deposit.

The mineralized zone is situated at the top of the Lower Extrusive I with overlying Lower Extrusives II. The ore can be classified into stockwork ore, massive ore and siliceous ore in ascending order. The gossanized zones consist of intensely weathered stockwork ore and siliceous ore in part. A detailed geologic survey and 12 drill holes were completed in the Hayl as Safil deposit area including gossan zones which showed rather high Au contents. The survey results delineated clear outline of the Hayl as Safil deposit. Based on the survey results, geologic map and sections were made as shown in Fig 1-10 and Fig. 1-11.

(2) Mineralized zones

The mineralized zones in Area A consist of four zones including two completely gossanized zones of Main Gossan and Small Gossan which are found on the surface, and two sulfide zones of the southeast of Main Gossan and north of Small Gossan which were confirmed by drilling.

(a) Main Gossan

Main Gossan occupies over an area of 300 m (N-S) by 240 m (E-W) in the center of Area A and forms a hill about 90 m high from the surface of terrace. The thickness of the gossan zone is estimated more than 90 m. The zone strikes ENE-WSW and dips 10° to 20° southward. Boundary between the gossan zone and underlying Lower Extrusives I is observed at the northern edge of Main Gossan. The boundary is clear due to different intensity of alteration. A small gossanised outcrop is found about 60 m south of Main Gossan. The Lower Extrusives II scatterly occurs between these gossanised zones, and gossanized mineralized zones were confirmed by drilling under this Lower Extrusives II. The Middle Volcanic Rocks consisting mainly of massive lavas are found at west of Main Gossan. A comparatively large-scale fault may exist between Main Gossan and the outcropping Middle Volcanic Rocks.

Faults trending NW-SE are predominant in the gossan zone. The Lower Extrusives II, found at the south of Main Gossan contacts with Main Gossan by a WNW-ESE trending fault. Sheared zones with one to two meters wide are found along this fault. The drill hole HS-39 completed by MPM in the middle of Main Gossan, encountered a mineralized zone with 20 m in thickness under 80 m thick Lower Extrusives I as shown on Fig. 1-11 (4). This fact may suggest the existence of a thrust fault between Main Gossan and the mineralized zone at southeast of Main Gossan. The result of the drill hole MJO-A6 completed in Phase I of this project also suggests the existence of the thrust fault.

The sulfide minerals in Main Gossan altered completely to limonite and goethite and no sulfide minerals are found in Main Gossan due to intense weathering. This mineralized zone is characterized with intense brecciation and silicification with quartz stockwork veins. The breccia consists of silicified volcanics, quartz-hematite, quartz, limonite, goethite and hematite. Brecciation occurred at least three or four times because re-brecciated breccias were found in many places. Matrix of the breccia is reddish brown and is mainly filled with hematite. Barren quartz veins of the latest stage cut the breccia. No significant differences are found throughout the gossan zone for the intensity of brecciation and composition of breccia. Quartz-hematite breccia tends to occur at the upper part, but some quartz-hematite breccia is also found in the middle and lower parts of the gossan zone. Enriched zone of secondary copper minerals are found in the Lower Extrusives II at south of Main Gossan and in the Lower Extrusives I just below Main Gossan. But the thickness of zone is one to two meters.

(b) Ore deposits at southeast of Main Gossan

This ore deposits was previously named the Hayl as Safil deposit. A total of 23 holes (3,551.15 m) was completed for this deposits before starting this project. Eleven holes totalling 1,740.80 m were carried out in the period of two years (Phase I and I) in this survey. During this period, MPM carried out seven holes totalling 1,108.80 m in this area based on the recommendation made by JICA/MMAJ. These holes confirmed thick stockwork ore zones.

This ore deposits is covered with thick terrace deposits except western part of the zone where a small gossanized zone outcrops. Drilling results show the mineralized zone is at the top of the Lower Extrusives I and is covered with the Lower Extrusives II. The size of this ore deposits is about 300 m (N-S) by 450 m (E-W) and extents northward below Main Gossan.

The ore deposits consist of stockwork, massive and siliceous ores in ascending order. Strongly chloritized zones with a few meters thick are found at the boundary between the ore deposits and footwall volcanic rocks. Argillized zone with gray clay occurs at the top of the deposits. The ore deposits are clearly bounded with these zones at the top and bottom. No sulfide minerals are found in the hanging wall and footwall volcanic rocks. The thickness of the ore deposits is more than 120 m at the northeren center of this zone. The mineralized zone increase the thickness for north, but the mineralization is going to weaken for north and magnetite which indicate marginal part of this type ore deposits in Oman is observed in the zone. This deposit is gossanized upto 40 m

in depth from the surface. The mineralized zone is situated at shallower depth in the western part of this zone and the zone is mostly gossanized. Soft minerals including limonite and clay etc. are eroded out by underground water and many caves are found in the gossanized zone.

This ore desposit consists mainly of stockwork ore and characterized by intense brecciation and silicification. The mineralization tends to weaken for north and contains magnetite in the stockwork zone. Strongly chloritized zones are found at the southern and eastern parts of this stockwork ore zone. Pyrite and hematite slightly tend to occur at the upper part of the stockwork zone, but no difference can be observed for copper concentration. Quartz-hematite breccias are found throughout this ore zone. The stockwork ore consists of strongly silicified, pyritized and chloritized breccia of volcanic rocks, and the matrix containing quartz and quartz-hematite veins with cholcopyrite and pyrite. This ore zone is re-brecciated and chalcopyrite-pyrite and quartz veinlets are found along fractures. Furthermore, sphalerite-pyrite-quartz veinlets cut the brecciated stockwork ore. The barren quartz veinlets of later stage also cut the ore zone.

Massive ore in the center of the orebody has gradational change to the stockwork ore zone. But volcanic rocks are intercalated between the massive and stockwork ore zone in the eastern part of the ore deposits. The thickness of the massive ore is a few meters in the center and more than 10 m at the eastern part, and the grade of Cu is very high (more than 6% Cu). Eastern margin of the massive ore zone is at the line through the drill holes HS-27 and MJO-A9. However, the drill hole MJO-A12 completed at 60 m east from this line encountered a massive ore zone of 3.30 m thick. This fact may suggest the existence of small local depression at the east and deposited massive sulfide ore. The massive ore generally shows more Au concentration. A part of the massive ore encountered by the hole of HS-14 shows more than 7 g/t Au. The contents of Au show good correlation with Cu contents in massive ore. Massive ore consists of breccia containing medium- to fine-grained pyrite and the matrix filled with pyrite-chalcopyrite. Minor beccias of siliceous ore and quartz-hematite are found in the massive ore. The breccia of massive ore contains colloform pyrite.

Siliceous ore is generally found above the massive ore zone and develops at the marginal parts of the ore deposits. Shape of the siliceous ore zone is irregular and some parts show more than 20 m in thickness. Siliceous ore consists of strongly brecciated and silicified volcanic rocks. Matrix of the breccia is white to gray clay and sulfide minerals. The ore is also cut by pyrite-quartz veinlets. Because the siliceous ore is found at the top of the orebody, the ore is usually affected by weathering and gossanization.

(c) Small Gossan

Small Gossan occurs about 300 m northwest of Main Gossan and forms a small corn-shape hill. This gossan covers an area of 120 m by 30 m. Several faults and fractures trending a NW-SW direction are found in the gossan zone.

No sulfide minerals are found in Small Gossan due to intense weathering. The zone is argillized and completely gossanized. The zone also presents strong silicification and brecciation and is more siliceous comparing with the zone of Main Gossan. Because of argillization, this zone may correspond to the siliceous ore. The matrix of breccia contains mainly hematite and limonite, but geothite is also observed in places.

(d) North of Small Gossan

This mineralized zone was confirmed by the drill hole of HS-7 which is 100 m away for north from Small Gossan and was completed by BRGM. The zone consists of massive ore with overlying argillized gossan zone. The massive ore encountered is shallow depth between 28.55 m and 42.25 m, and the average grade is 3.69% Cu. The gossan zone above the massive ore shows similar nature of Small Gossan and this gossan zone continues to Small Gossan. Additional drill holes completed by BRGM did not confirm the extensions of the mineralized zone and encountered the thrust fault at the northern end the orebody.

(3) Gold in gossanized zone

If gold contents in the gossanized zone are high, planning for mine development should include this factor. Therefore, sampling from gossan zone and drill cores were carried out and assayed them. Locations for the samples collected from Main Gossan and Small Gossan are shown in Fig. 1-12, and the results of assaying including drill cores are given in Table 1-2.

Assaying for the drill hole HS-39 was made by MPM. The results show no significantly gold concentrated zones. The best intersection (D.L. 0.90 m, 5.4 g/t Au, 12.9 g/t Ag) in the hole MJO-A10 at the depth from 25.60 m to 26.50 m.

Because no highly Au concentrated zones are observed and generally low grade of Au, the gossanized zones may have no potentiality. The zones should be treated as waste in the stage of pre-stripping for mine development.

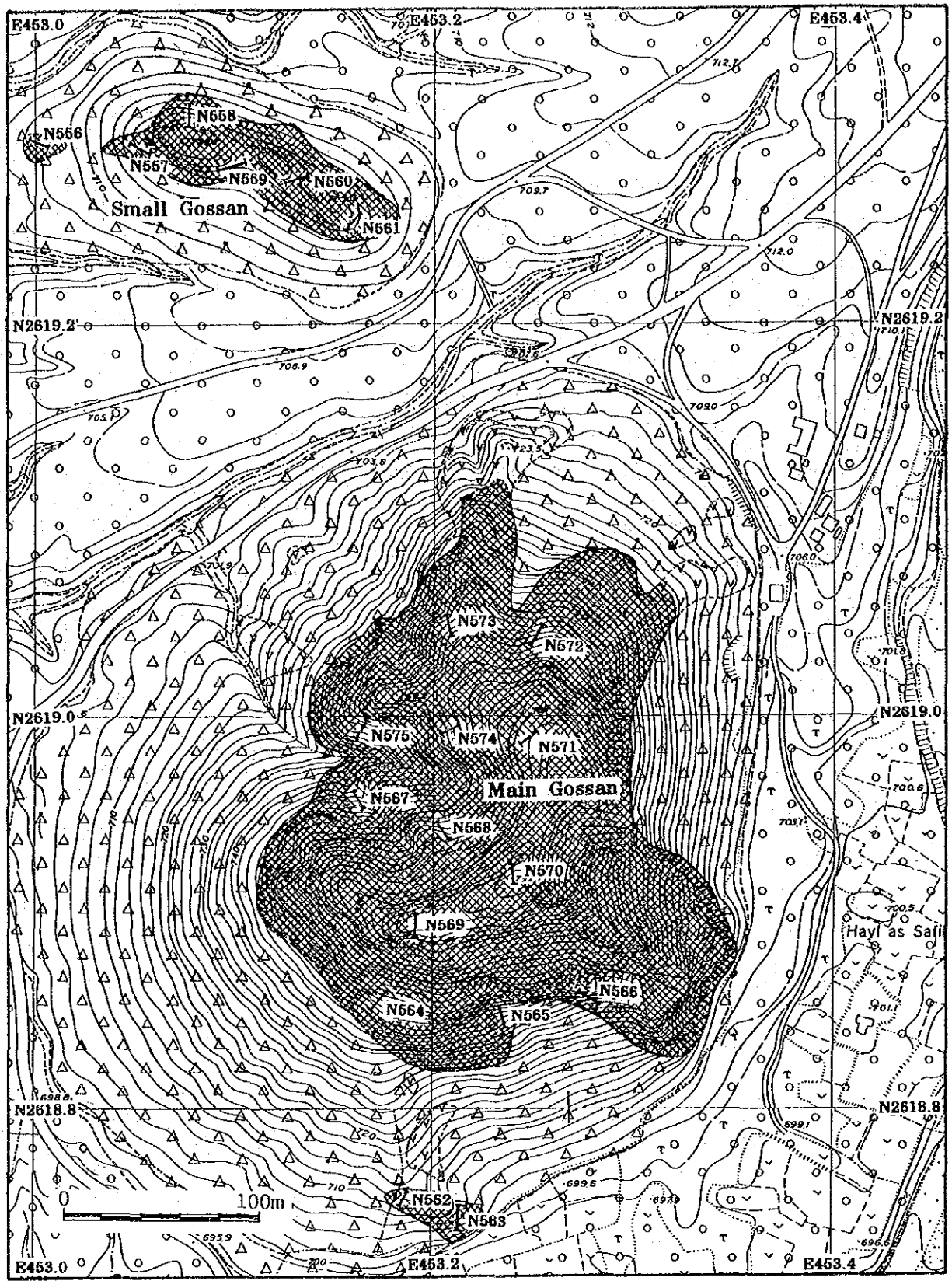

Fig. 1-12 Location map of samples collected from gossan zones for assaying in area A

Table 1-2 Assay results for gossan samples in Area A

Gossan sample

Sample number	Descriptions	Assay results			
		Au(g/t)	Ag(g/t)	Cu (%)	Zn (%)
N556	Small Gossan. Siliceous gossan. Porous and dark to reddish brown. Limonite, goethite and hematite.	0.8	3.3	0.19	0.01
N557	Small Gossan. Siliceous gossan with clay. Hematite breccia dominant. Intensely brecciated.	Tr	Tr	0.15	<0.01
N558	Small Gossan. Siliceous gossan. Quartz stockwork veinlets dominant.	0.2	0.9	0.06	<0.01
N559	Small Gossan. Siliceous gossan. White to whitish brown. Limonite, hematite and goethite.	Tr	Tr	0.05	<0.01
N560	Small Gossan. Siliceous gossan. Whitish brown quartz with limonite and hematite breccia.	Tr	Tr	0.06	<0.01
N561	Small Gossan. Siliceous gossan. Quartz network zone with dominant hematite breccia and minor limonite.	Tr	Tr	0.07	<0.01
N562	South of Main Gossan. Siliceous gossan with minor limonite and hematite.	0.8	4.2	0.02	<0.01
N563	South of Main Gossan. Siliceous gossan with limonite hematite and goethite.	0.4	1.2	0.08	<0.01
N564	Main Gossan. Siliceous gossan with dominant hematite breccia. Intensely brecciated.	Tr	Tr	0.06	<0.01
N565	Main Gossan. Siliceous gossan with hematite breccia and limonite. Intenselybrecciated.	1.5	19.1	0.03	<0.01
N566	Main Gossan. Siliceous gossan with hematite breccia and minor limonite. Intensely brecciated.	1.2	10.1	0.06	<0.01
N567	Main Gossan. Siliceous gossan with minor goethite and hematite.	0.2	0.6	0.06	<0.01
N568	Main Gossan. Siliceous gossan with dominant hematite breccia and minor limonite and goethite.	Tr	Tr	0.04	<0.01
N569	Main Gossan. Siliceous gossan, porous. Dominant limonite and minor hematite.	1.4	3.0	0.03	<0.01
N570	Main Gossan. Siliceous gossan with hematite breccia and minor limonite.	0.8	6.0	0.03	<0.01
N571	Main Gossan. Siliceous gossan with limonite, hematite and goethite.	Tr	Tr	0.02	<0.01
N572	Main Gossan. Siliceous gossan with minor limonite and hematite.	Tr	Tr	0.14	<0.01
N573	Main Gossan. Siliceous gossan with hematite and limonite.	Tr	Tr	0.06	<0.01
N574	Main Gossan. Siliceous gossan with goethite, hematite and limonite.	0.1	0.7	0.05	<0.01
N575	Main Gossan. Siliceous gossan with dominant limonite and minor hematite and goethite.	Tr	0.4	0.20	0.02

Drill core sample

Hole No.	Depth (m)	Drilled length (m)	Au(g/t)	Ag(g/t)	Cu (%)	Zn (%)
MJO-A7	12.80 ～ 29.80	17.00	0.17	0.86	0.38	0.07
MJO-A10	7.20 ～ 37.90	30.70	0.57	4.50	0.11	<0.01
MJO-A11	28.20 ～ 42.30	14.10	1.07	6.52	0.16	0.01
HS-39	0.55 ～ 44.30	43.75	0.11	0.16	0.12	0.02

1-2-4 Petrochemical studies

(1) Purpose and methodology

The survey was carried out to clarify the nature of the Samail Volcanic Rocks which played important roles for formation of Cyprus-type copper deposit in the area and to examine the possibility to classify the volcanic sequence petrochemically. Because stratigraphically same volcanic rocks are found in both the areas of Area A and B, the studies were carried out using all samples collected in both the areas.

Thirty samples were used for whole rock analyses of 13 major components and 33 samples were chemically analyzed for 24 elements. The samples were mostly collected from the Samail Ophiolite. The results of the chemical analyses of whole rock and minor elements, and the norm calculation are given in Appendix 2. Locations of sampling site are given by UTM grid on the tables in Appendix 2. Detection limits for Al, Ca, Fe, Mg, P, K, Na and W are 10 ppm, Bi and Pb are 3 ppm, Mo is 2 ppm and Ag is 0.1 ppm. Other than these element, the detection limits are 1 ppm. The chemical analyses were made in the Geotecnical Laboratory of Bishimetal Exploration Co., Ltd. The analyses were conducted by ICAP (Induced Coupled Argon Plasma Emission Spectrophotometer) method except Ag, K and Na. The atomic absorption method was adopted for Ag and, K and Na were analysed by the flame spectrometory method.

(2) Results of studies

(a) Cumulate Sequence (Cg) and High-level Gabbro (Hg)

One sample each of Cumulate Sequence and High-level Gabbro was analyzed. Among the major components and minor elements, SiO_2 contents (48.23% ~ 48.28%) as well as Al_2O_3, MnO, P_2O_5, Co, Ni, Pb, Ag and Zn show similar values for these two samples. However, MgO, CaO, Cr and Ni are rich in Cumulate Sequence. Fe_2O_3* (* : total), Na_2O, Ki_2O, V, Zn and incompatible elements including TiO_2, P_2O_5, Ba and Sr are comparatively poor, so that small differentiation between them can be recognized. In addition, their solidification indices (S.I. = 53.59, 66.96) show higher value than those of Sheeted-dyke Complex and Samail Volcanic Rocks. FeO*/MgO ratios (F.M.I. = 0.37, 0.63) show comparatively low value due to more contents of MgO.

(b) Sheeted-dyke Complex (Sd)

Two samples of Sheeted-dyke Complex show basaltic in SiO_2 contents (51, 52%). The rocks are relatively rich in FeO*, CaO, TiO_2, V and Sr and relatively poor in MgO, Cr and Ni compared with High-level Gabbro. The range of values is almost same to Lower Volcanic Rocks. The Sheeted-dykes show the lowest contents of Cu.

(c) Lower Volcanic Rocks (L)

Eleven samples from the Lower Extrusives I and nine samples from the Lower Extrusives II of the Lower Volcanic Rocks were analyzed.

Lower Extrusives I (LI)

SiO_2 contents (46 ~ 61%) of the rocks range from basaltic (45 ~ 52% SiO_2) to andesitic (53 ~ 66% SiO_2). The contents of Fe_2O_3* (6 ~ 12%), MgO (5 ~ 12%), CaO (1 ~ 6%) and most of minor elements of the Lower Extrusives I range wider than the Lower Extrusives II and Middle Volcanic Rocks (M). However, the rocks are rich in FeO_3*, TiO_2, Cr, Co, W and Zn and have a tendency of poor in MgO, CaO and Cu. F.M.I. values (FeO*/MgO ratio) ranging from 0.64 to 1.80 and S.I. (consolidation index) values show wide range from 26 to 59.

Lower Extrusives II (LII)

SiO_2 contents of the rocks range from 49% (basaltic) to 57% (andesitic). The contents of major components show narrower range than that of the Lower Extrusives I. Fe_2O_3* (6% ~ 9%), TiO_2 (0.2% ~ 0.5%) are relatively poor and Na_2O (2.2% ~ 5.6%) is relatively rich. On the minor elements, the rocks have a tendency of slightly richer in Ni, poor in Co and relatively poor in Cu, V and Zn in comparison with the Lower Extrusives I.

F.M.I. value (0.88 ~ 1.47) and S.I. value (28 ~ 44) of the rocks are mostly within the same range to the Lower Extrusives I.

(d) Middle Volcanic Roks (M)

Four samples from this unit show basaltic to andesitic values of SiO_2 ranging from 47% to 55%. In general, the rocks show a tendency of richer in incompatible elements (TiO_2, P_2O_5), Fe_2O_3* and Cu and relatively poor in MgO, K_2O, Co, Ni, Sr and Cr. And then, the rocks tend to rich in MnO, Co, Cr, Ni and Zn in comparison with the Lower Volcanic Rocks.

F.M.I. value (1.01 ~ 1.67) and S.I. value (29 ~ 37) of the rocks indicate to be rich in Fe and poor in Mg.

(e) Late dyke

Two samples of Late dyke were analyzed. SiO_2 content (50.32%, 54.77%) shows basaltic and andesitic. The rocks are generally rich in TiO_2, Fe_2O_3*, P_2O_5 and poor in MgO, CaO, Cu and Cr. These tendencies mostly correspond with the Middle Volcanic Rocks, so that the Late dyke and Middle Volcanic Rocks are inferred to be same origin. The rocks tend to be richer in TiO_2, Na_2O, K_2O, BaO, Cu and Zn and poor in CaO, MnO, MgO and Sr in comparison with the Sheeted-dyke Complex. F.M.I.value (1.73, 1.88) is high and S.I. value (25, 34) is relatively low.

(3) Discussion

The rocks of the Rakah area are generally undergone alteration and metamorphism, so that it is necessary to examine petrochemically by stable components and elements against alteration and metamorphism. In general, incompatible elements including Ti, P, Zr and Y are considered to be immobile elements. TiO_2 - FeO*/MgO and P_2O_5 - FeO*/MgO diagrams are shown in Fig. 1-13. TiO_2 and P_2O_5 increase gently together with increasing FeO*/MgO ratio which is used to the scale of differentiation of magma. Therefore, it is thought that TiO_2 and P_2O_5 are incompatible components to some degree. And then, the relationship between TiO_2 and P_2O_5, which is shown in Fig. 1-14, shows positive correlation, which indicates that these components are not affected relatively by alteration and metamorphism (Ocean-floor metamorphism). Consequently, it can be calculated the influence of alteration and metamorphism between TiO_2 and other components. Right angle diagrams of TiO_2 versus other components are given in Appendix 3. Relatively well concentrated components, which is thought to be less affection of alteration and metamorphism, are SiO_2, FeO*, MnO, P_2O_5, Ni, Cr, V and Zn. Slightly scattered components in the diagrams, which are relatively affected by alteration and metamorphism, are Al_2O_3, MgO and Cu. On the other hand, CaO, K_2O, Na_2O, Pb, Sr, Ag and Ba are scattered in the diagrams due to alteration and metamorphism, so that these components are not suitable to use for petrochemical examination.

Variation diagrams of immobile components and FeO*/MgO ratio, which is used generally as a scale of the differentiation, are shown in Appendix 4 and Fig. 1-13. Following to increase of FeO*/MgO ratio, SiO_2, FeO*, TiO_2, P_2O_5 and V enrich gently and MgO, Cr, Ni and Cu deplete. The differentiation of the whole rocks do not reach to the maximum of TiO_2 (around 3.0 in FeO*/MgO ratio). This tendency corresponds with the SiO_2 contents (43 ~ 57%) and microscopic observation results. The Cumulate Sequence, High-level Gabbro, Sheeted-dyke Complex and Lower Volcanic Rocks are roughly plotted along one trend in TiO_2-FeO*/MgO diagram (Fig. 1-13) as well as FeO*-FeO*/MgO, MgO-FeO*/MgO (Appendix 4) and TiO_2-P_2O_5 diagrams (Fig. 1-14), so that it suggests that these rocks are sequential fractionations from same magma.

Lower Volcanic Rocks consist of Lower Extrusives I and overlying Lower Extrusives II. Syngenetic sedimentary deposits are formed at the top of the Lower Extrusives I and are covered by the Lower Extrusives II. Petrochemical correlation between them suggest sequential fractionations, because the ranges of the components mostly overlap each other. However, the Lower Extrusives II has a tendency of rich in Ni and Cr and slightly poor in Co, TiO_2 Fe_2O_3*, Cu and V. It indicates to be a fractionation of early stage of the differentiation. The diagrams of Co versus Cr, Cu and V (Fig. 1-15) show relatively clear differences of plotted domains of them and it is possible to discriminate between them.

On the other hand, the Middle Volcanic Rocks and Late dyke, which are thought to be same origin, are characterized by slightly poor in TiO_2, P_2O_5, Cr, Ni and Co and different domain plotted in SiO_2-FeO*/MgO and FeO*-FeO*/MgO diagrams in comparison with the Lower Volcanic

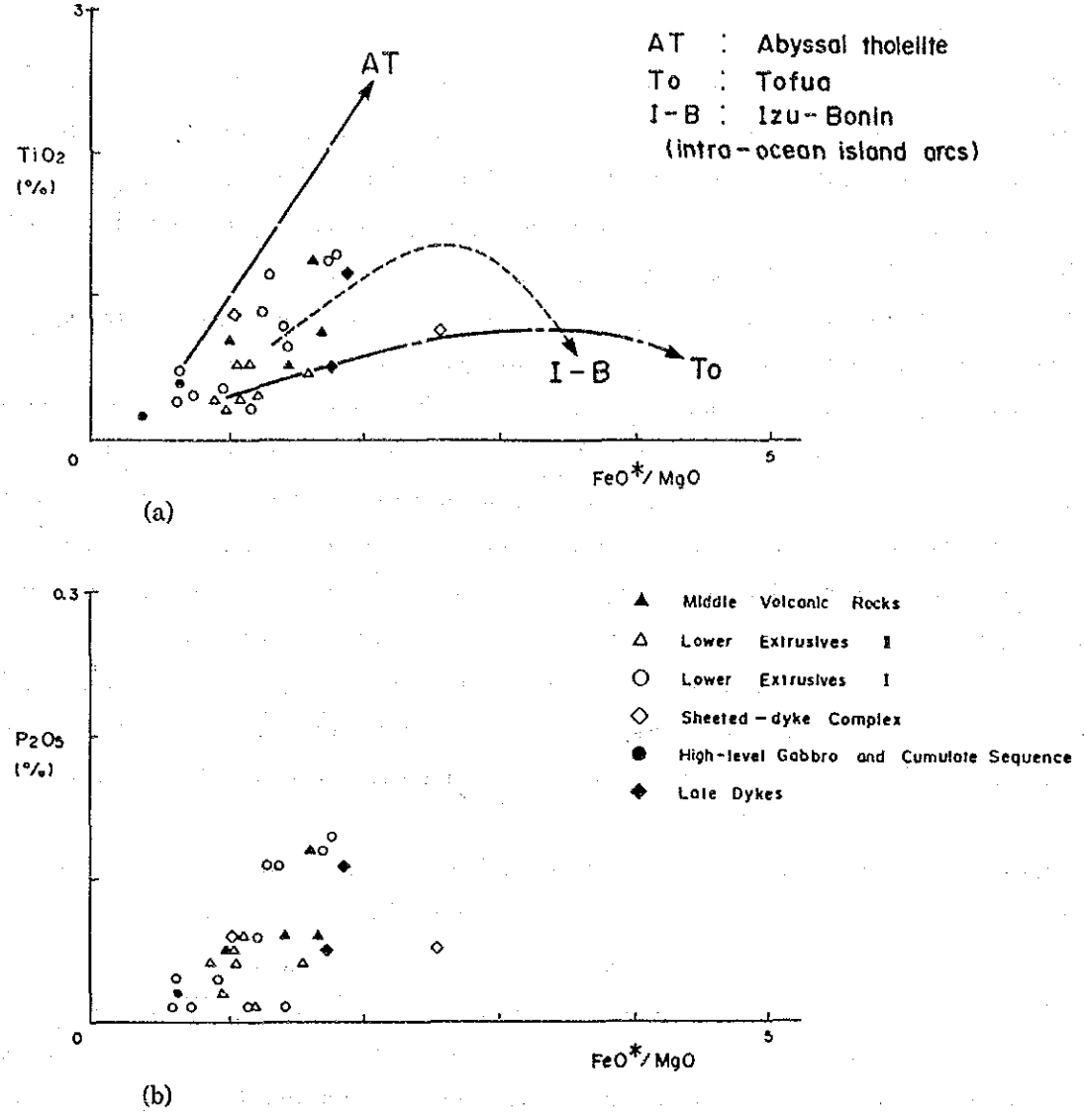

Fig. 1-13 TiO_2-FeO*/MgO and P_2O_5-FeO*/MgO diagrams

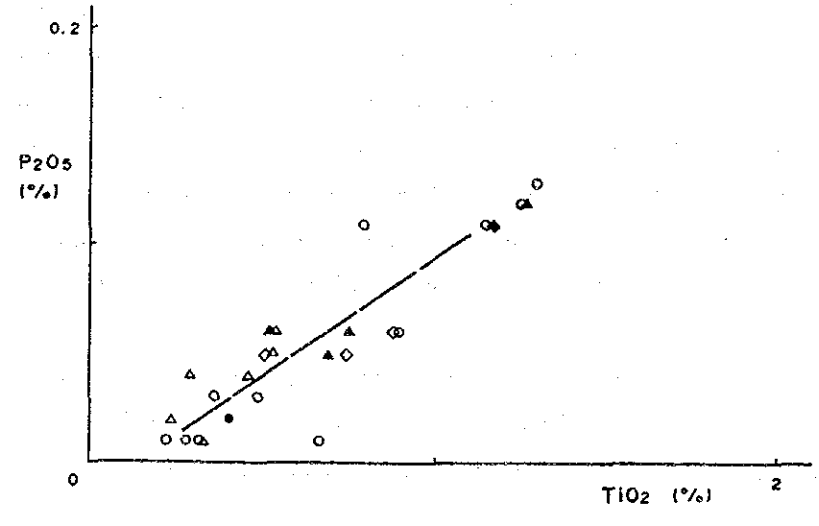

Fig. 1-14 P_2O_5-TiO_2 diagram

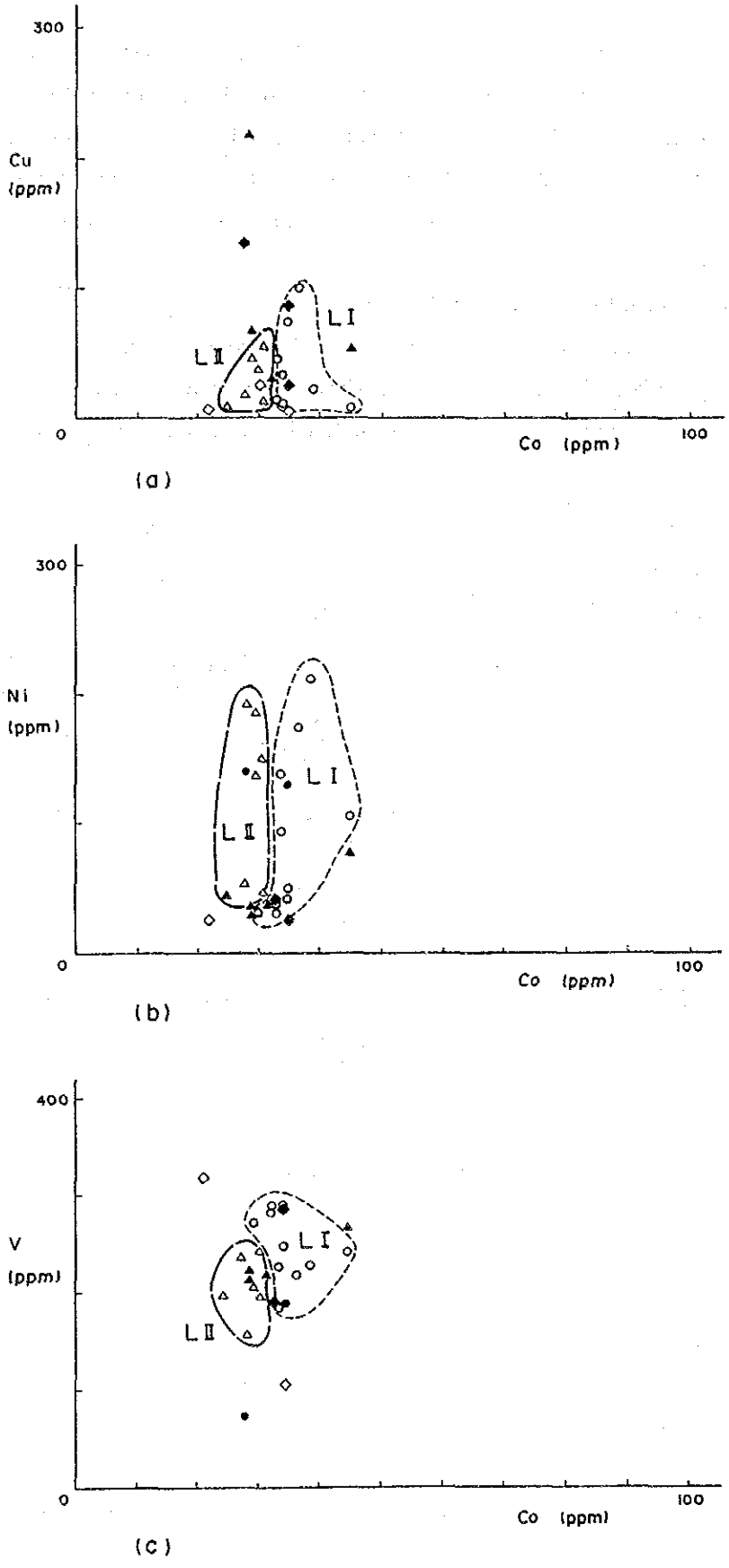

Fig. 1-15 Cu-Co, Ni-Co and V-Co diagrams

Rocks, Sheeted-dyke Complex and Gabbros.

The differential trends of these rocks are shown in TiO_2-FeO*/MgO diagram (Fig. 1-13), AMF diagram (Fig. 1-16) and FeO*-FeO*/MgO diagram (Appendix 4). The Lower Volcanic Rocks are plotted at the domain of Abyssal tholeiite and Island-arc tholeiite series, but the Middle Volcanic Rocks are plotted at the domains of the Island-arc tholeiite series and Calc-alkali series in local. This fact suggests that the Lower Volcanic Rocks and Middle Volcanic Rocks were formed by different magmatism.

This study concluded that the Lower Extrusives I and II were possibly formed by the same magmatism, but the magma which formed the Lower Extrusives II were more primitive. Two different magmatisms form the Lower Volcanic Rocks and the Middle Vpolcanic Rocks separately. These results are same as the results of studies completed in the Sohar area (Bishimetal, 1987).

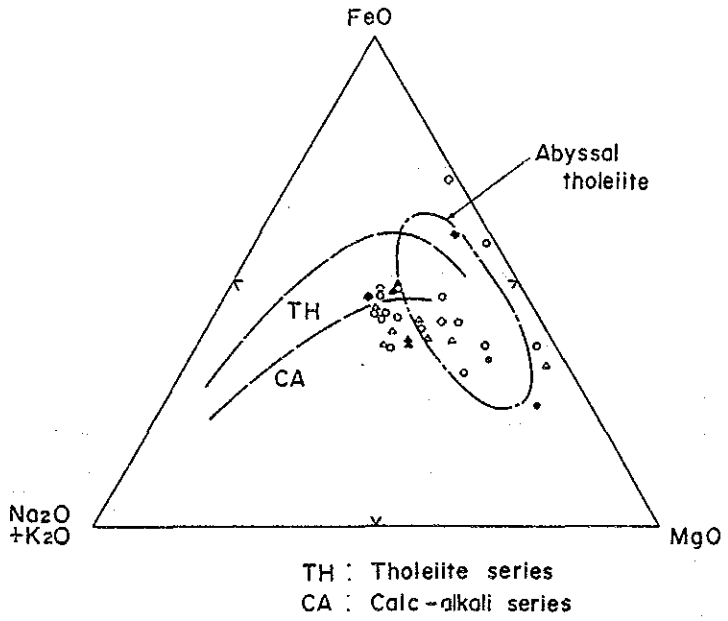

Fig. 1-16 AMF diagram

1-3 Geophysical survey

In order to delineate an extension of the Hayl as Safil deposit and to obtain the guideline of the further drilling survey, Charged Potential (CP) survey was conducted in Phase I covering Area A (3 km^2).

1-3-1 Suvey method

(1) Outline of Charged Potential Method

Charged Potential (CP) method is an electrical-exploration method, in which one current electrode (C1) is positioned in a conductor either in outcrop or in a borehole. The other current electrode (C2) is a great distance away and the potential electrodes (P1) are moved about with the area for mapping the mineral deposits. In this method, a far current electrode (C2) is commonly placed more than 4 km away from charging point (C1) in a such manner as that C1 acts like a mono-pole. And a far potential electrode (P2), utilized as a standard potential point (0 mv), is placed also 4 km away from charging point (C1) either at the opposite side of C2 or at the middle point between C1 and C2.

Schematic illustration of this method is given in Fig. 1-17.

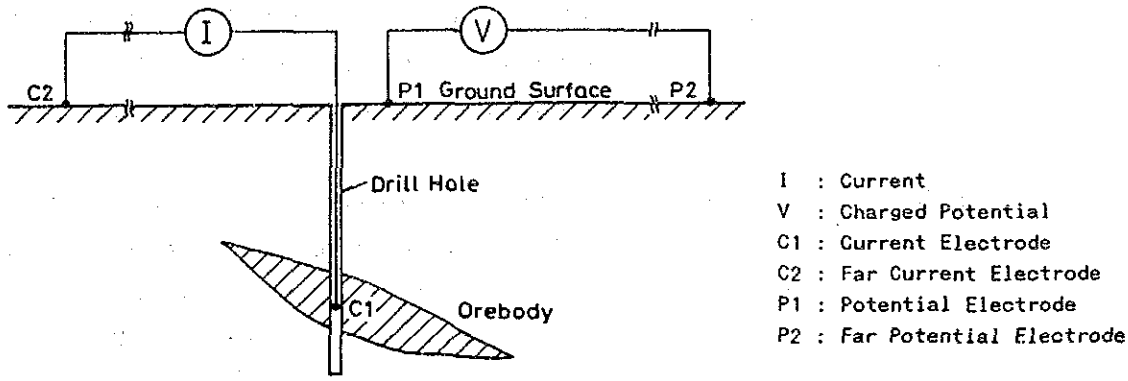

Fig. 1-17 Schematic illustration of charged potential method

This method is also called mise-a-la-masse method and/or excitation-at-the-mass method. And this method is commonly utilized in the mineral exploration and recently adopted in the geothermal exploration to delineate the distribution of the geothermal reservoir.

Fig. 1-18 (a) illustrates a charged potential distribution showing a concentric circle pattern, when current is introduced at one point in the homogenous earth. When r is the distance between

C1 and P1, r' is the distance between an image of C1 and P1, ρ is the resistivity of the earth, and I is a charging current, the charged potential (V) at P1 is given by the following equation:

$$V = (\rho I/4\pi) \cdot (1/r + 1/r')$$

While, Fig. 1-18 (b) shows the potential distribution, when current electrode is placed in a conductor (orebody). In this illustration, charged potential distribution shows a pattern suggesting the extension of the conductor (orebody).

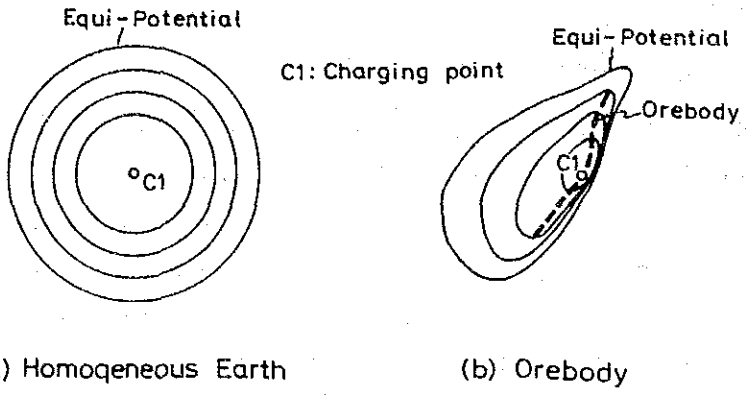

(a) Homogeneous Earth (b) Orebody

Fig. 1-18 Model distribution patterns of charged potential

(2) Measuremement

The 611 CP stations in total were settled at 50 m and 100 m apart each in an area of 3 km^2, by means of the open traverse surveying method. The location of measuring points are shown in Fig. 1-19. Coordinates of each of CP stations in meters was decided by settling the origin (0, 0) at X=N2619.00 and Y=E453.00, and by setting positive directions towards the south and the east, respectively.

Although, at the beginning of the geophysical survey, the charging point (C1) was planned to be positioned in the MJ0-A4 hole, C1 was placed in the neighbouring HS-14 hole, because the thickness of the massive orebody hit by the MJ0-A4 hole was very thin. And another charging point (C1) was set in the HS-7 drill hole which hit the north orebody located near Small Gossan, in order to clarify the continuation between the Hayl as Safil and north orebody.

Current electrode	Drill hole	Depth of electrode	Remarks
Charging point (C1)	HS-14	103 m	Southeast of Main Gossan
	HS-7	38 m	North of Small Gossan
Far current electrode (C2)	MJO-B5	115 m	Rakah deposit

A far potential electrode (P2) was settled at Wadi Rakah, 4 km south of the middle point (N2614.7, E455.1) between Area A and B.

By means of introducing an alternative DC (0.1 Hz) current of 1.6 A through 2.5 A between two current electrodes, C1 and C2, charged potential at each CP station (P1) was measured in mV.

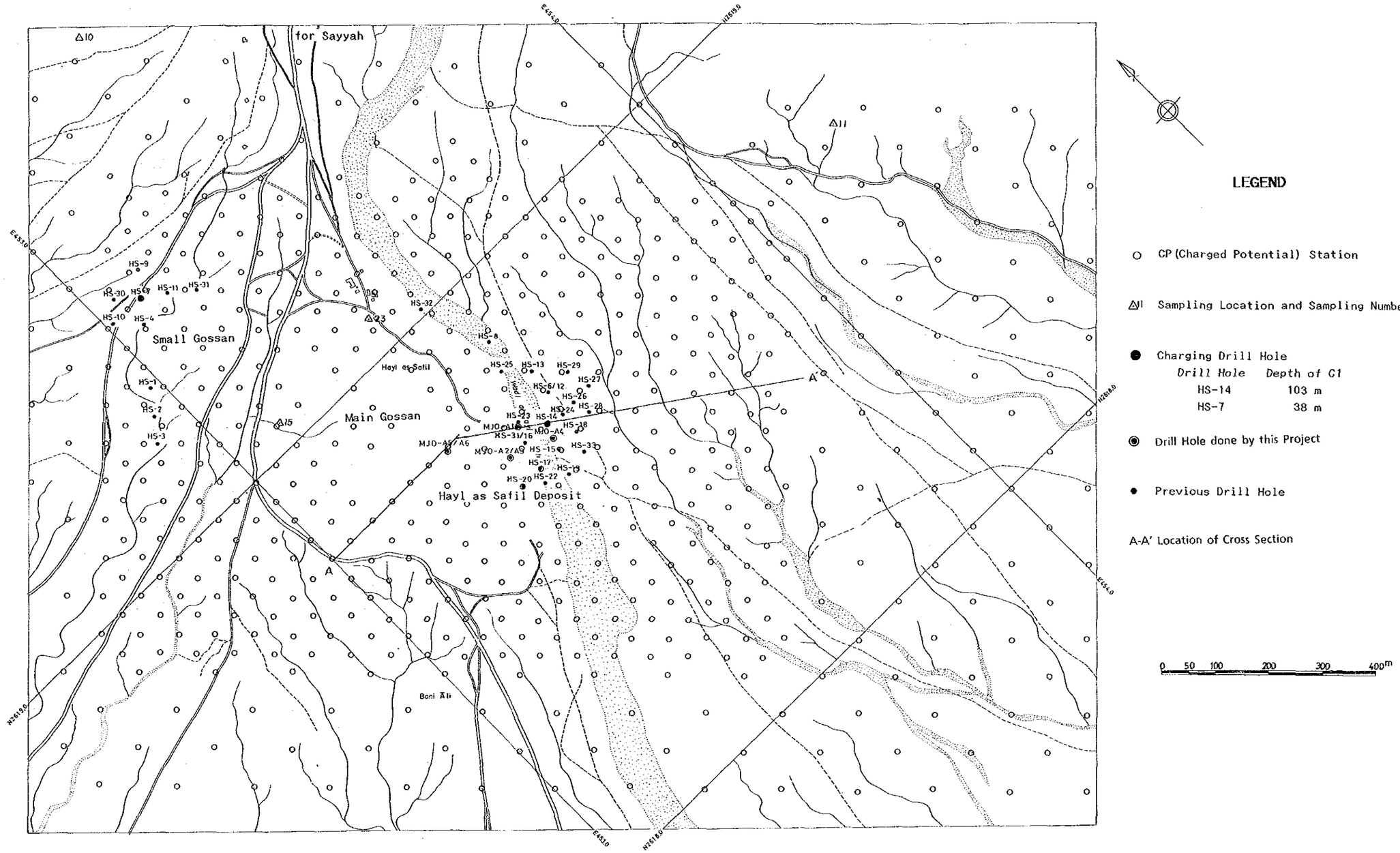

Fig. 1-19 Location map of CP survey stations in Area A

(3) Survey instrument

Survey instruments adopted for this survey are as follows:

Instrument	Model	Manufacturer	Specification	Amount
Transmitter	CH-T7801	Chiba Electronics Co. (Japan)	Output; 800 V/3 A/0.1 Hz	1 pc
Receiver	Model 27	John Fluke MFG Co. (U.S.A.)	DC voltage; 0.01 mV to 1 kV	3 pcs
Engine Generator	GPU-2000	Geonics Inc.	Output; 2 kW/115 V/1φ/3φ	1 pc

(4) Data arrangement and analyses

Charged potentials in mV/A at each CP station were obtained by means of dividing measured potentials in mV by current in A. And the plan map of the charged potential was made for each of the two drill holes.

On the charged potential map, the highest potential is shown above and/or near the charging point (current-introduced drill hole), and charged potentials decrease towards the whole directions, showing the distortions which suggest the extension of the conductor including orebody. However, it is very difficult to estimate the boundary of the conductor from this map only. Electric field (E) is given by the following equation:

$$|E| = |\partial\phi/\partial h|$$

Where, ϕ is the charged potential, and h is the unit normal vector to equi-potential line.

The extreme values of the electric fields coincide with the boundary of the conductor, as shown in Fig. 1-20. Therefore, the plan map of the electric fields was made for each charging hole.

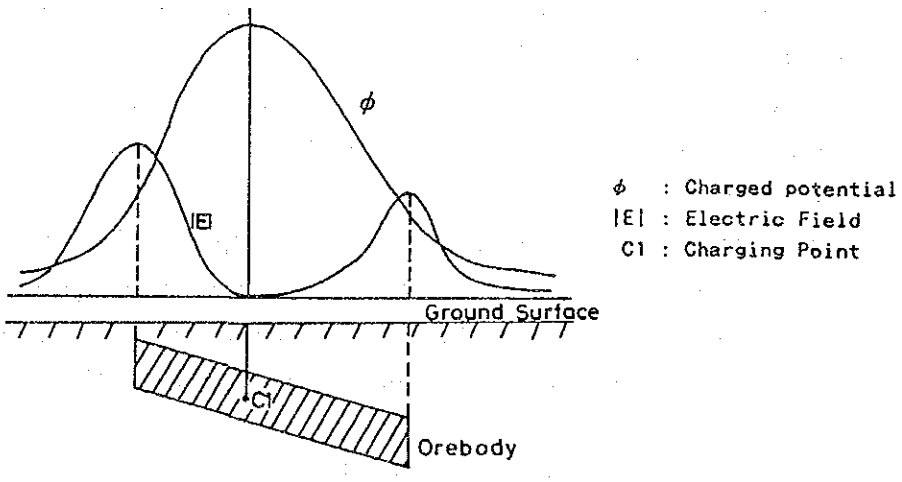

Fig. 1-20 Model curve of charged potential and its electric field

The above two kinds of plan maps are utilized to delineate the distribution of the conductor qualitatively. On the other hand, the quantitative delineation of the conductor is done by two-dimensional (2-D) model simulation using 2-D finite element method. The procedure of 2-D model simulation is as follows:

① A profile running through the current-introduced drill hole is chosen.
② Taking the results of the drilling survey and the physical property tests into consideration, the 2-D resistivity model structure is constructed.
③ Charged potential curve for the 2-D resistivity model is calculated and compared with the observed potential curve.
④ If the difference between the observed and calculated curves is a little, the calculation is terminated. If the difference is large, the 2-D model structure is reconstructed and model calculation is repeated until the calculated curve matches the observed curve.

Based on the above-mentioned method, the survey results in Area A were analysed. The charged potentials and electric fields at each CP station are shown in Appendix 5 and 6, respectively. The plan maps of charged potentials due to two drill holes, HS-14 and HS-7 are shown in Fig. 1-21. The plan map of electric fields due to these two holes, HS-14 and HS-7 are shown in Fig. 1-22 and Fig. 1-23, respectively.

1-3-2 Results of survey

(1) Results of physical property test

The 24 samples, in total, of rocks and ores collected in the both areas, Area A and B, were used for the physical property tests. Each of samples was collected at the ground surface and/or from drill cores. Sampling locations of rock samples collected at the ground surface are shown in Fig. 1-19.

Three kinds of physical properties, resistivity, PFE and phase difference, of each rock/ore sample were measured by means of the Spectral IP testing system made by Zonge Engineering and Research Organization Inc. (U.S.A.). The results of the physical property tests were analysed together for the samples collected in both the areas of Area A and B because of their same geologic setting. The results of the test are shown in Table 1-3.

Physical properties in wet condition were tested. Physical properties of rock/ore samples are not necessarily same as those existed in the earth, but they may show similar values.

Average values of physical properties for the geologic units and/or ores are shown in Table II-1-4 in which the resistivity shows the descending order of gossan > Lower Extrusives II (LII) > Lower Extrusives I (LI) > stockwork ore > massive ore.

Therefore, it is expected that the current charged in the orebody flows in the massive and stockwork orebodies concentratedly because resistivities of those orebodies are extremely lower than those of the surrounding rocks, and the charged potentials show a distribution pattern

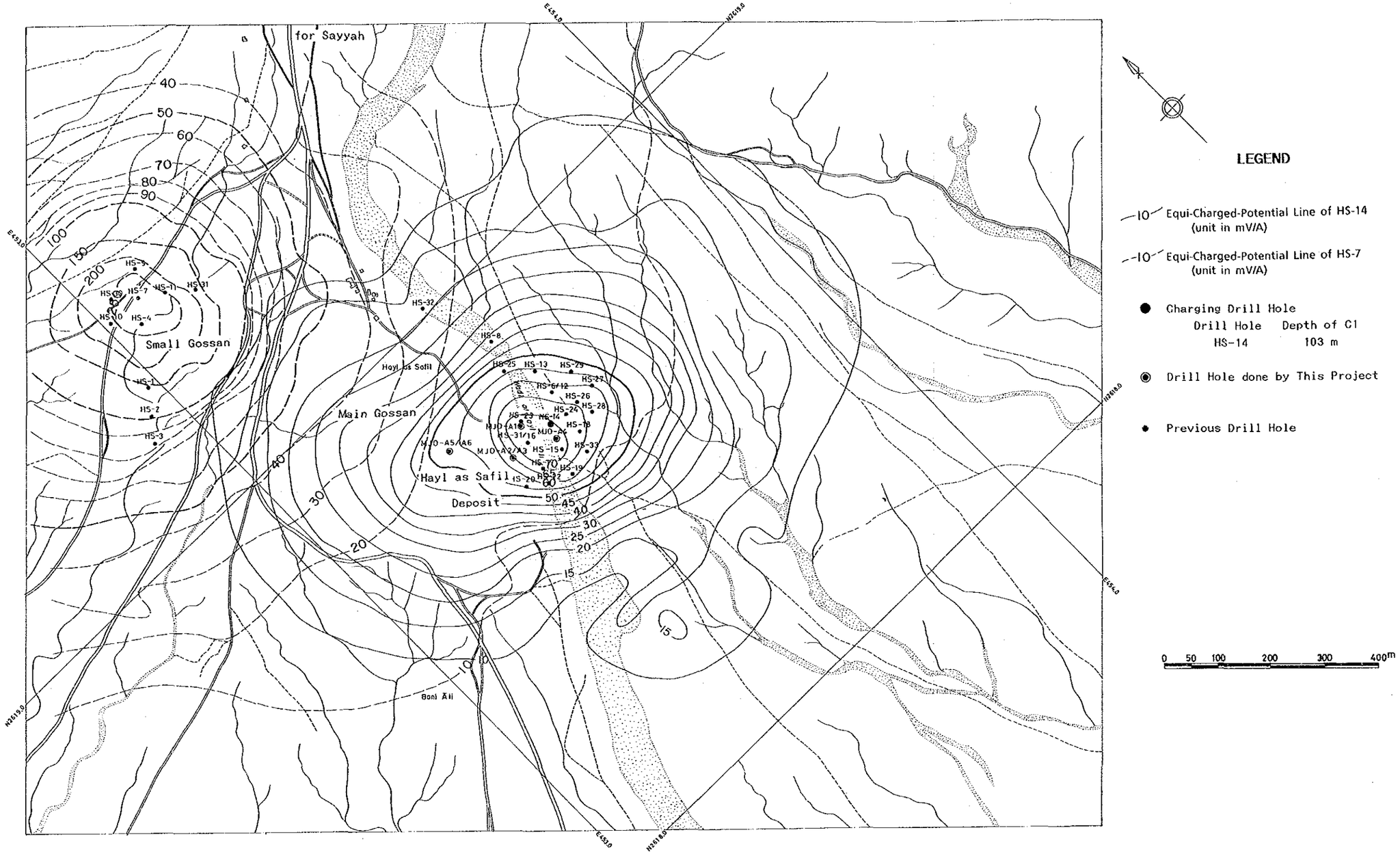

Fig. 1-21 Charged potential map for the drill holes HS-14 and HS-7 in Area A

Fig. 1-22 Electric field map for the drill hole HS-14 in Area A

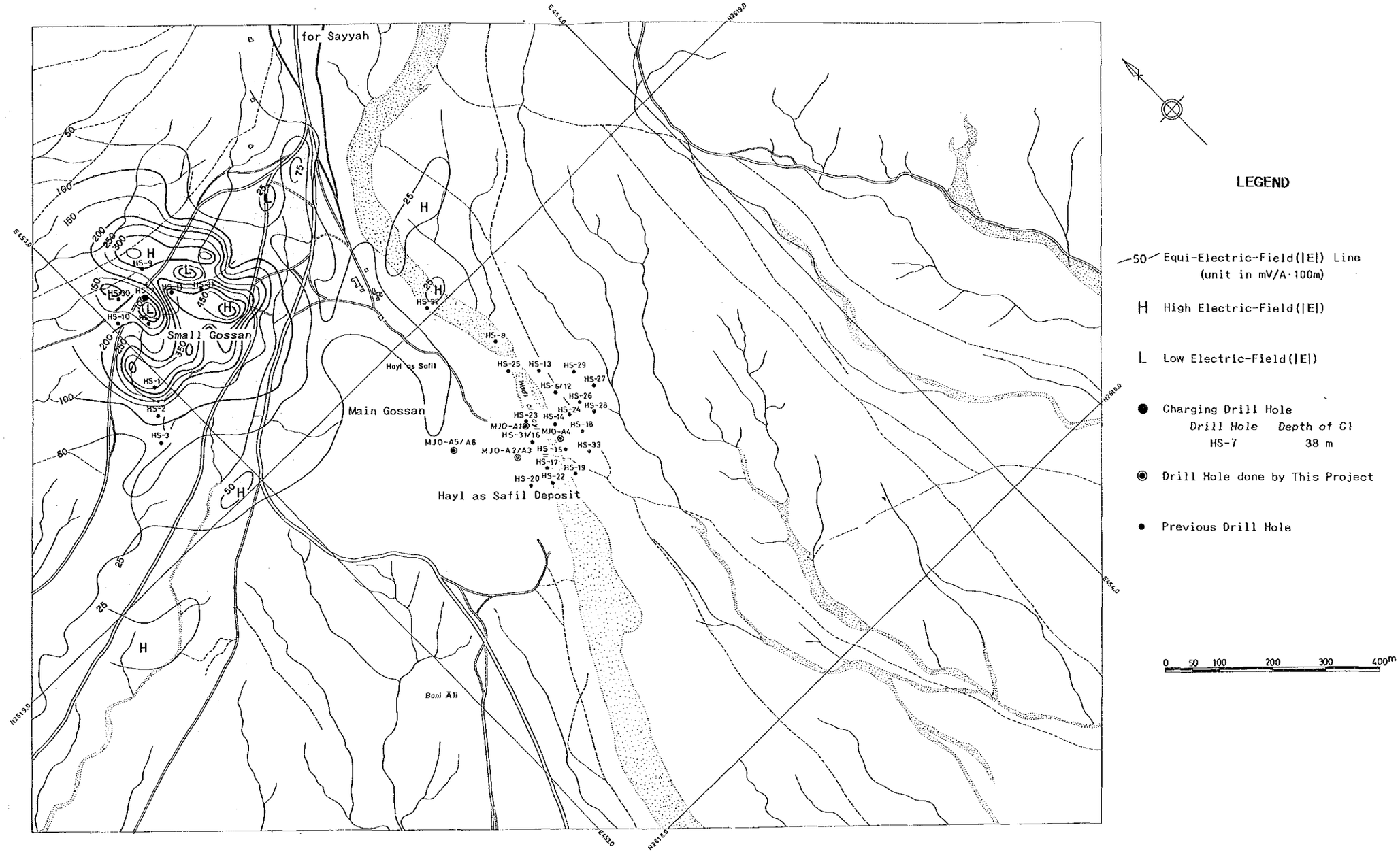

Fig. 1-23 Electric field map for the drill hole HS-7 in Area A

Table 1-3 Values of physical properties

Sample No.	Area name	Drill hole	Sampled depth(m)	Descriptions	Resistivity (Ω·m)	PFE (%)	Phase difference (-mrad)
1	A	MJO-A2	136.00	Pillow lava (LI)	963	0.3	2
2	B	MJO-B3	133.60	Pillow lava (LI)	878	10.4	94
3	B	MJO-B3	147.70	Pillow lava (LI)	545	0.5	3
4	B	MJO-B4	101.20	Pillow lava (LI)	191	0.2	1
5	B	MJO-B5	107.60	Pillow lava (LI)	731	6.0	53
6	B	MJO-B5	136.10	Pillow lava (LI)	1,380	1.2	7
7	B	MJO-B6	85.90	Pillow lava (LI)	545	0.5	3
Average values of Lower Extrusives I					747	2.7	23
8	A	MJO-A1	63.70	Pillow lava (LII)	366	0.2	1
9	A	MJO-A4	44.20	Massive lava(LII)	580	0.5	2
10	A	—	—	Pillow lava (LII)	2,450	1.6	10
11	A	—	—	Pillow lava (LII)	154	0.5	4
12	B	MJO-B2	52.20	Pillow lava (LII)	4,190	0.9	6
13	B	MJO-B3	55.20	Pillow lava (LII)	1,810	0.9	5
14	B	MJO-B3	80.10	Pillow lava (LII)	583	2.7	18
15	A	—	—	Pillow lava (Me)	957	4.3	19
Average values of Lower Extrusives II					1,390	1.5	8
16	A	MJO-A1	82.60	Stockwork ore	4.25	62.9	370
17	A	MJO-A1	92.30	Stockwork ore	14.8	37.3	259
18	A	MJO-A4	89.30	Stockwork ore	91.4	32.3	216
19	B	MJO-B5	47.70	Stockwork ore	9.12	33.6	251
20	B	MJO-B5	69.00	Stockwork ore	5.97	64.6	389
Average values of stockwork ore					25.1	46.1	297
21	A	MJO-A1	78.40	Massive ore	1.26	4.9	46
22	A	MJO-A4	81.20	Massive ore	0.97	18.5	159
Average values of massive ore					1.12	11.7	103
23	A	—	—	Gossan	1,930	2.5	16
24	A	—	—	Gossan	3,500	0.5	4
Average values of gossan					2,715	1.5	10

reflecting the shape of the orebody.

(2) Charged potentials

Two charged potential maps due to HS-14 and HS-7 gave different distribution patterns and suggested that the orebodies confirmed by the drill holes, HS-14 and HS-7, were separated.

(a) Charged potentials due to HS-14

A charged potential plan map due to charging point placed at the depth of 103 m in the HS-14 drill hole is shown in Fig. 1-21.

On this plan map, the highest peak of charged potential of 73.5 mV/A is found at the west of HS-14 hole, and the equi-charged potential lines extend towards the west (the south of Main Gossan), the southeast and the northeast. These distribution patterns seem to reflect the distribution of the Hayl as Safil deposit.

The northern and southwestern boundaries of conductor including orebody are presumed at 200 m north and 200 m southwest of HS-14 hole, respectively, where the large gradients of charged potentials are observed.

A distortion of the equi-potential lines extends only up to the southern-half part of Main Gossan toward the west, and does not continue to Small Gossan. Therefore, it is thought that both of the Hayl as Safil and the north orebody are insulated electrically, that is, there is no continuation between both orebodies.

(b) Charged potentials due to HS-7

A charged potential plan map due to charging point placed at the depth of 38 m in the HS-7 drill hole is shown in Fig. 1-21.

On this plan map, a highest peak of charged potential of 592 mV/A is found at 50 m south of HS-7 hole, and charged potentials show a distribution of a little extension in a N-S direction. A higher charged-potential value at the highest peak than that due to HS-14 hole is only due to shallower charging point (C1) and not due to the difference of the sizes of the deposits.

The boundaries of conductors including orebody are presumed around 150 m north, east, south and west of HS-7 hole, respectively, where large gradients of charged potentials are observed. At the south of HS-7 hole, the southern boundary seems to be located at the southern edge of Small Gossan, and the equi-potential lines do not extend toward Main Gossan. Therefore, the both of the Hayl as Safil and the north orebody seem to be insulated on this map also.

(3) Electric fields

As described in 1-3-1 (4), low $|\mathbf{E}|$ (intensity of electric field) anomalies are distributed in the distribution area of the conductor including orebody, and high $|\mathbf{E}|$ anomalies on the boundary of the conductor. Utilizing the characteristics of $|\mathbf{E}|$ distribution, the boundary of

conductor including orebody could be estimated. While, low and high | E | anomalies are called when the some points show relatively low or high | E | comparing with the neighbouring points.

(a) Electric fields due to HS-14

The electric fields due to HS-14 is shown in Fig. 1-22. On this map, several low | E | anomalies are distributed around the HS-14 hole, and are surrounded by notable high | E | anomalies. The boundary of the conductor including orebody seems to be located at 200 m west (100 m west of MJ0-A3 hole at the western bank of wadi), at 200 m north (around HS-8 hole), at 200 m southeast and 100 m south of the HS-14 hole. And the boundary at the northwestern edge near MJ0-A5/A6 holes extends 50 m towards the west.

Moreover, high | E | anomalies extend towards the northwest (the southern-half of Main Gossan), northeast and southeast, and the existence of the conductor is expected at these portions. However, since the | E | are lower than those in above notable anomalies, the conductor in each of these three portions seems to become either thinner or deeper or highly resistive.

In the main part of the conductor as described above, there are found the equi - | E | lines trending in NW-SE, WNW-ESE and N-S directions, which may reflect the directions of the fault structures.

The | E | distribution due to HS-14 hole shows no relation between the Hayl as Safil and north orebody, as shown in the charged potentials (Fig. 1-17).

(b) Electric fields due to HS-7

The electric fields due to HS-7 hole is shown in Fig. 1-20.

On this map, a low | E | anomaly with a center at 50 m west of HS-7 hole, is distributed around the HS-14 hole, and are surrounded by notable high | E | anomalies.

Judging from the distribution of high | E | anomalies, the boundary of the conductor including orebody is located at the southern fringe of Small Gossan, around 100 m east of HS-7 hole, around 100 m north of HS-7 hole and around 150 m west of HS-7 hole. Therefore, it is suggested that there is no continuity between the Hayl as Safil and North deposits.

(4) Model simulatoin

In order to evaluate western and southeastern extensions of equi-potential lines on a charged potential plan map due to HS-14 hole, 2-D (two-dimensional) model calculation by means of 2-D finite element method was applied. Location of 2-D section line, running at the HS-14 hole, is shown in Fig. 1-19. The section line runs through HS-14 hole in NW-SE direction. At the north of HS-14 hole, the line extends to 30 m east of MJ0-A5 hole and toward the west through MJ0-A5 hole. The results of the calculation is shown in Fig. 1-24.

The initial model was constructed on the basis of the results of the drilling survey and the physical property test of the drill holes on and/or near the section line such as HS-14, MJ0-A5, etc.

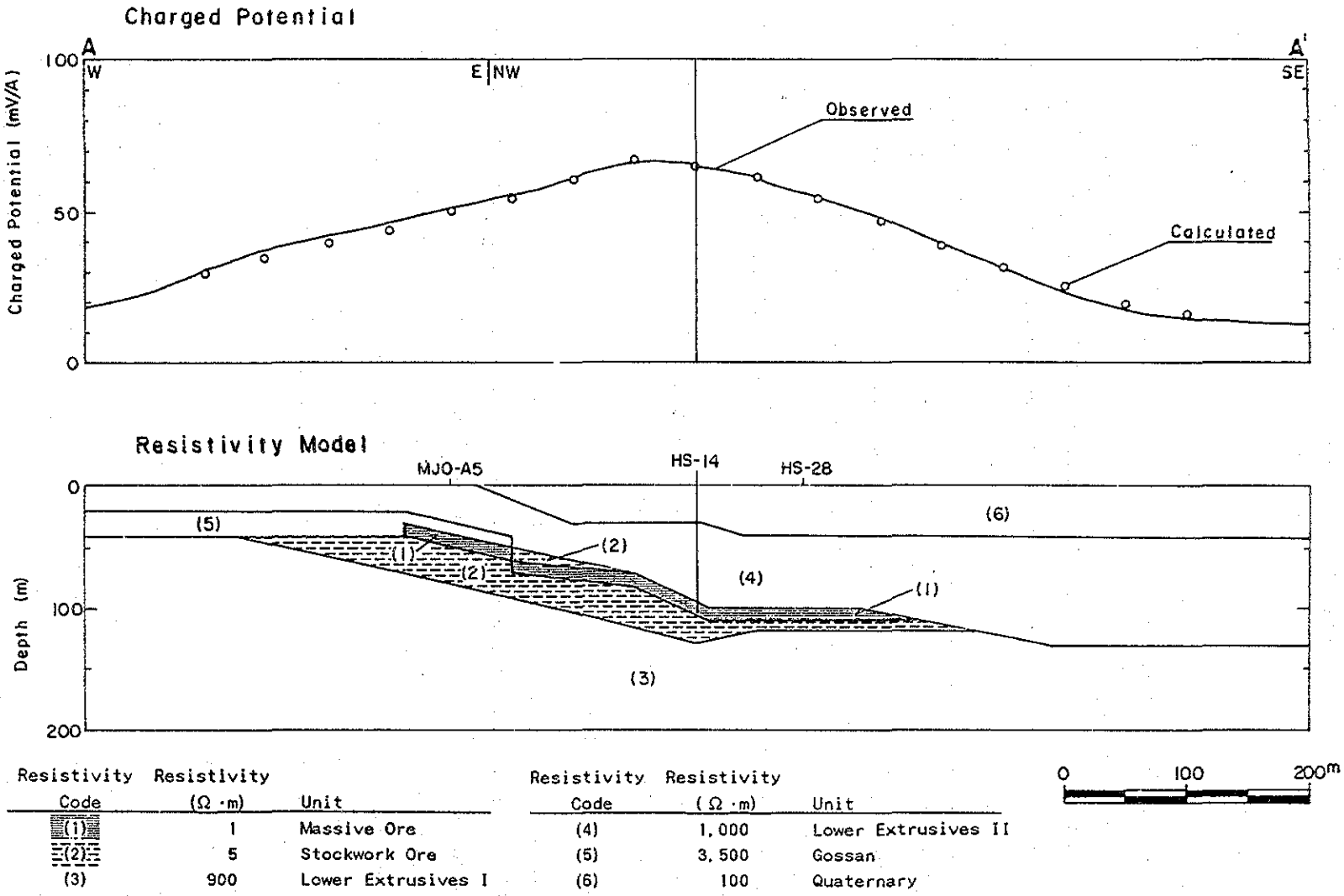

Code	Resistivity (Ω·m)	Unit
(1)	1	Massive Ore
(2)	5	Stockwork Ore
(3)	900	Lower Extrusives I
(4)	1,000	Lower Extrusives II
(5)	3,500	Gossan
(6)	100	Quaternary

Fig. 1-24 Results of model calculation and its resistivity structure for the Hayl as Safil deposit

By means of setting each hole as a control point model calculation was repeated by changing the resistivity and thickness of resistivity model structure, until the calculated potential curve matches the observed curve.

Resistivity of each formation and orebody of the final model is 1 Ω · m for massive ore, 5 Ω · m for stockwork ore, 900 Ω · m for Lower Extrusives I (LI), 1,000 Ω · m for Lower Extrusives II (LII), 3,000 Ω · m for gossan and 100 Ω · m for terrace deposits of Quaternary sediments.

The orebody including massive and stockwork ore zones is distributed at the thickness of 20 m through 50 m, around 200 m southeast of HS-14 hole toward the southeast and around 200 m west of MJ0-A5 hole toward the west, and is diminished at the both ends. Within the orebody, the massive ore zone is distributed between 50 m west of MJ0-A5 hole and 150 m southeast of HS-14 hole at the thickness of about 10 m.

A high resistivity layer of 3,500 Ω · m with the thickness of 10 m to 20 m, corresponding to gossan, is distributed at the west of MJ0-A5 hole, and a resistivity of 100 Ω · m with the thickness of 30 m to 40 m, corresponding to terrace deposits, is also distributed at the surface at the southeast of HS-14 hole.

(5) Summary of geophysical survey results

A geophysical interpretation map is shown in Fig. 1-25. The main part of the Hayl as Safil deposit, evaluated by the geophysical survey results, is distributed with the width of 250 m in N-S and E-W directions each, and extends to 200 m southeast of HS-14 hole. And the boundary of the main part is assumed around 20 m through 60 m west of MJ0-A5/A6 holes at the west bank of the wadi, around 20 m north of HS-8 hole, around 140 m east of HS-14 hole, and around HS-19 hole. At the northwestern edge of the main part, the MJ0-A5/A6 holes were drilled and hit the massive and stockwork orebody successfully, so that this drilling survey results seem to encourage the geophysical survey results.

In this main part, the distribution of the orebody is controlled by the fault structures running in NW-SE and WNW-ESE directions, and the orebody seems to be distributed at relatively large thickness.

According to the geophysical survey results, the orebody extends toward the northwest (the southern-half part of Main Gossan) and to 50 m west of the western edge of the main part, and in these extensions the thickness of the orebody seems to be thin. And also the northeastern extension of the orebody, which is distributed toward 360 m northeast of HS-14 hole, seems to be existed in the depth. The north orebody, which is distributed at the width of 200 m in N-S and E-W directions each and shows a southern edge at southern fringe of Small Gossan, is thought not to continue to the Hayl as Safil deposit.

Fig. 1-25 Geophysical interpretation map of Area A